Hatfield Marine Science Center
Dynamic Revetment Project
DSL permit # 45455-FP

Monitoring Report
February, 2015

February 11, 2015

Submitted by:
Robert Cowen, Director
Hatfield Marine Science Center
Oregon State University
Robert.Cowen@oregonstate.edu
541-867-0211

Editor:
Walt Nelson, US Environmental Protection Agency

Contributors:
Beach Profiles:
Jonathan Allan, Oregon Department of Geology and Mineral Industries

Fish:
Scarlett Arbuckle, Oregon State University
Heppell Laboratory, Oregon State University

Benthic Invertebrates and Vegetation:
Christina Folger, US Environmental Protection Agency
Walt Nelson, US Environmental Protection Agency

Summary

Stabilization of the Yaquina Bay shoreline along the northeastern edge of the Hatfield Marine Science Center (HMSC) campus became necessary to halt erosion that threatened both HMSC critical infrastructure (seawater storage tank) and public access to the HMSC Nature Trail. A Dynamic Revetment (gravel beach) was installed in November, 2011 on 260 feet of shoreline to mitigate erosion. Shoreline topographic and biological monitoring was initiated before and has continued after the project completion. Monitoring of beach profiles indicated that as of January 2015, the 2011 Dynamic Revetment Project (DRP) has generally successfully stabilized the shoreline in the project area. Beach profile data also indicated that the 2007 DRP continued to be successful in stabilizing further retreat of the shoreline. In both areas, some loss of gravel at the top of the shore profile due to overtopping of the beach during highest tides was noted, and some additional placement of gravel at these locations is recommended. Rapid erosion has continued in the adjacent Reference beach area and over the period 2009-2015 has been as great as 11 m (36 ft). The erosion in the Reference area adjacent to the south end of new gravel beach appears entirely a function of antecedent erosion that is taking place along the entire length of this shore and is not related to any end effects associated with the expanded gravel beach.

Monitoring of beach wrack invertebrates, fish, and vegetation was conducted in 2014. Per unit of beach wrack biomass, the density of wrack invertebrates was significantly greater in the DRP area as compared to both the 2007 DRP area and the Reference area. Total amount of beach wrack was much sparser in the Reference area because of vertical beach scarps generated by erosion that appeared to limit wrack accumulation. As has been a consistent pattern, fish were significantly more abundant in the Reference area compared to the DRP. However, this pattern was present in the pre-project sampling, and the Reference area may have a higher degree of physical habitat complexity, resulting from root masses of trees that have been eroded onto the shore. Chum salmon were recorded from both the DRP and Reference area in 2014 in approximately equal numbers. Preliminary assessment of fish using stationary GoPro® camera samples suggested that there is active fish usage of the DRP gravel shoreline. Sampling issues continue to be problematic for quantitative comparisons of fish abundance. As has consistently been observed, vegetation coverage was significantly greater and presence of non-living substrata was significantly less in the Reference area as compared to the DRP. These differences are consistent with pre-project site differences, probably resulting from a low area of the shoreline which allows increased flooding and associated disturbance in the DRP back shore area. Fish and wrack invertebrates, such as beach hoppers, continue to utilize the DRP project area. Biological differences in fish and vegetation observed in the post-project monitoring in 2014 tended to reflect differences in habitat that were present before the DRP project.

Table of Contents

1.0 HMSC Beach and Shoreline Monitoring

1.1 Background

Stabilization of the Yaquina Bay shoreline along the northeastern edge of the Hatfield Marine Science Center (HMSC) campus became necessary in 2007 to halt erosion that threatened both HMSC critical infrastructure (seawater storage tank) and public access to the HMSC nature trail. The Hatfield Marine Science Center (HMSC) Estuary trail was constructed in 1988 and is unique to Newport since it provides the only trail for exploring the Yaquina Bay estuary from its banks, as well as being one of the longer accessible trails in the area for those with disabilities. Since the late 1990s/early 2000 the trail has experienced erosion from a combination of oceanographic processes including high frequency wind waves coupled with high tides and tidal currents associated with both the ebb and flood tide.

Among the range of solutions to coastal erosion, gravel beaches have long been recognized as an effective form of natural coastal protection, minimizing the potential for inundation from wave overtopping as well as exhibiting a remarkable degree of stability in the face of sustained wave attack (van Hijum, 1974; Nicholls and Webber, 1988; Allan et al., 2005; Komar and Allan, 2010). This is due to their high threshold of motion and because of the asymmetry (shape) of shoaling waves and swash velocities on the beach face, which results in a greater propensity for onshore particle movement compared with sand-size particles, forming a steeply sloping beach face. Once formed, the porous gravel beach is able to disrupt and dissipate the incident-wave energy, even during intense storms. As a result of these characteristics, artificially constructed gravel beaches have been suggested as a viable approach for protection from coastal erosion, variously termed “cobble berms” or “dynamic revetments” when used in such applications. Once formed, the gravel beach is considered to be dynamic in that the gravels may be moved about by waves and currents, adopting a morphology that will reflect those assailing forces. Gravel beaches are considered a “soft” form of coastal engineering to help mitigate erosion.

In 2006, the Oregon Department of Geology and Mineral Industries (DOGAMI) assisted HMSC with the design of a dynamic revetment project. The project was completed in March 2007 with the assistance of the Oregon Army National Guard IRT program and resulted in the stabilization of approximately 200 linear feet of the northeastern shoreline of HMSC. That shoreline section has remained stable since dynamic revetment implementation. Erosion continued at a lower rate to the south of the 2007 project area, but in the winter of 2009-2010, weather conditions resulted in rapid erosion of up to 13 ft along approximately 500 linear ft of shoreline. This erosion moved the shoreline to the edge of the nature trail in one location, and to within only 25 ft of portions of the seawater system infrastructure for HMSC. The seawater system supports the research of Oregon State University and the five federal and state agency programs co-located on site. The threat to critical public infrastructure required an additional erosion control effort utilizing the gravel shoreline technique.

Therefore, on November 10-11, 2011, an additional 260 ft of gravel beach was installed with the assistance of the Oregon Army National Guard. As a condition of the permit for installation, Oregon Department of State Lands required a monitoring program be put in place to assess both the geological performance and the biological impacts of the gravel beach installation (herein termed Dynamic Revetment Project or DRP). This report constitutes the fourth annual report on the monitoring program, representing three full years after project completion.

2.0 Physical Parameters
2.1 Beach Profile Survey Methodology

Beach profiles that are orientated perpendicular to the shoreline can be surveyed using a variety of approaches, including a simple graduated rod and chain, surveying level and staff, Total Station theodolite and reflective prism, Light Detection and Ranging (LIDAR) airborne altimetry, and Real-Time Kinematic Differential Global Positioning System (RTK-DGPS) technology. Traditional techniques such as leveling instruments and Total Stations are capable of providing accurate representations of the morphology of a beach, but are demanding in terms of time and effort. At the other end of the spectrum, high-resolution topographic surveys of the beach derived from LIDAR are ideal for capturing the 3-dimensional state of the beach, over an extended length of coast within a matter of hours. However, the LIDAR technology remains expensive and is impractical along small segments of shore, and more importantly, the high costs effectively limits the temporal resolution of the surveys and hence the ability of the end-user to understand short-term changes in the beach morphology.

Within this range of technologies, the application of RTK-DGPS for surveying the morphology of both the sub-aerial and sub-aqueous portions of the beach has effectively become the accepted standard [e.g. Ruggiero et al., 2005; Allan and Hart, 2008], and has been the surveying technique used in this study. The Global Positioning System (GPS) is a worldwide radio-navigation system formed from a constellation of 24 satellites and their ground stations, originally developed by the US Department of Defense; in 2007 the Russian Government made their GLONASS satellite network available increasing the number of satellites to ~46 (as of February 2011). In its simplest form, GPS can be thought of as triangulation with the GPS satellites acting as reference points, enabling users to calculate their position to within several meters (e.g. using inexpensive off the shelf hand-held units), while survey grade GPS units are capable of providing positional and elevation measurements that are accurate to a centimeter. At least four satellites are needed mathematically to determine an exact position, although more satellites are generally available. The process is complicated since all GPS receivers are subject to error, which can significantly degrade the accuracy of the derived position. These errors include the GPS satellite orbit and clock drift plus signal delays caused by the atmosphere and ionosphere and multipath effects (where the signals bounce off features and create a poor signal). For example, hand-held autonomous receivers have positional accuracies that are typically less than about 10 m (<~30 ft), but can be improved to less than 5 m (<~15 ft) using the Wide Area Augmentation System (WAAS). This latter system is essentially a form of differential correction that accounts for the above errors, which is then broadcast through one of two geostationary satellites to WAAS enabled GPS receivers.

Greater survey accuracies are achieved with differential GPS (DGPS) using two or more GPS receivers to simultaneously track the same satellites enabling comparisons to be made between two sets of observations. One receiver is typically located over a known reference point and the position of an unknown point is determined relative to that reference point. With the more sophisticated 24-channel dual-frequency RTK-DGPS receivers, positional accuracies can be improved to the sub-centimeter level when operating in static mode and to within a few centimeters when in RTK mode (i.e. as the rover GPS is moved about). In this study we used Trimble© 24-channel dual-frequency R7/R8 GPS receivers. This system consists of a GPS base station (R7), Zephyr Geodetic antenna (model 2), HPB450 radio modem, and R8 "rover" GPS (Figure 2.1). Trimble reports that both the R7/R8 and 5700/5800 GPS systems have horizontal errors of approximately ±1-cm + 1ppm (parts per million * the baseline length) and ±2-cm in the vertical (Trimble, 2011).

To convert a space-based positioning system to a ground-based local grid coordinate system, a precise mathematical transformation is necessary. While some of these adjustments are accomplished by specifying the map projection, datum and geoid model prior to commencing a field survey, an additional transformation is necessary whereby the GPS measurements are tied to known ground control points. This latter step is called a GPS site calibration, such that the GPS measurements are calibrated to ground control points with known vertical and horizontal coordinates using a rigorous least-squares adjustments procedure. Performing the calibration is initially undertaken in the field using the Trimble TSC2 GPS controller and then re-evaluated in the office using Trimble's Business Office software (v2.5).

Survey control at HMSC was provided by occupying two benchmarks established by National Geodetic Survey (NGS – Hamilton and 943 5380 tidal), and by the Coastal Field Office of DOGAMI (hmsc-crk & hmsc-pth). Coordinates assigned to these monuments were derived using a combination of approaches that included the Online Positioning User Service (OPUS) maintained by the NGS (http://www.ngs.noaa.gov/OPUS/) and the Oregon Real Time GPS Network (http://www.theorgn.net/) established by the Oregon Department of Transportation.

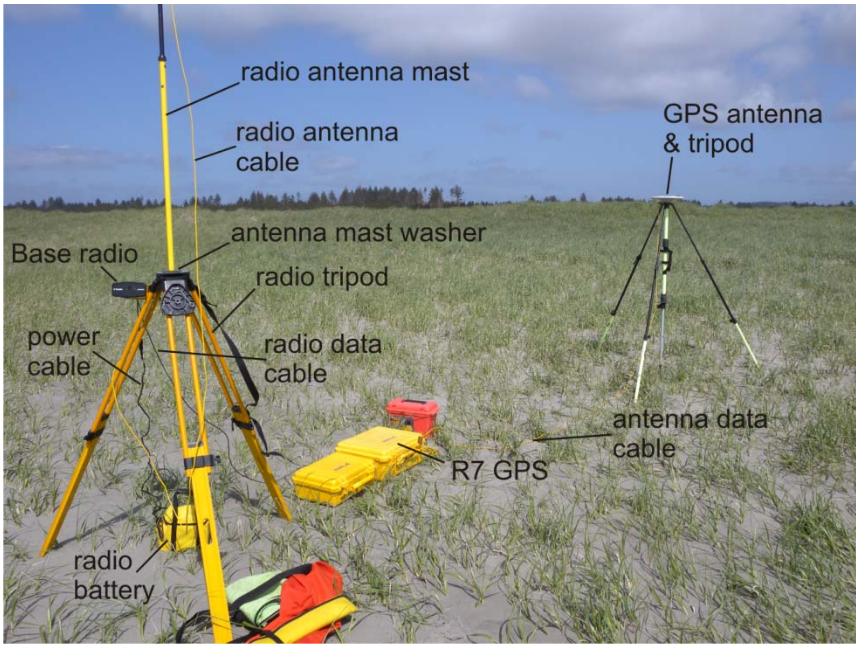

Figure 2.1. The Trimble R7 base station antenna in operation on the Clatsop Plains. Corrected GPS position and elevation information is transmitted by an HPB450 Pacific Crest radio to the R8 GPS rover unit.

2.2 Beach Profile Results

For the purposes of this study, we established 15 beach profile transect lines along the estuary trail (Figure 2.2), which extends from the HMSC wharf in the northwest, southward approximately 290 m (~950 ft). Of these, 5 of the lines were originally established in May 2006 (1-5) to document changes on the original gravel beach constructed there in late 2006, while the remaining 10 lines were established in July 2011. An additional 3 transect lines were established in May 2014 (Table 2.1), expanding the monitoring network further to the south (Figure 2.2).

GPS Surveys were undertaken on the original profile 1-5 lines in May 2006, March 2007 and in September 2007 (Table 2.1). These data have been supplemented with high resolution terrain elevations extracted from a LIDAR dataset (8 points per m^2) collected by DOGAMI for the Northern Oregon coast in July 2009. Table 2.1 presents the times when all surveys of the beach were carried out. As described in previous reports, subsequent future surveys will be confined to mid-late winter (~February/March timeframe) and in late summer (~September).

Table 2.1: Dates when beach surveys and mapping efforts were undertaken

Measurement Date	Type	Transects
May 19 2006	RTK-DGPS	1-5
March 16 2007	RTK-DGPS	1-5
September 6 2007	RTK-DGPS	1-5
July 19 2009	LIDAR	1-15
July 13 2011	RTK-DGPS	1-15
December 19 2011	RTK-DGPS	1-15
January 13 2012	RTK-DGPS	1-15
May 7 2012	RTK-DGPS	1-15
December 21 2012	RTK-DGPS	1-15
May 5 2013	RTK-DGPS	1-15
August 19 2013	RTK-DGPS	1-15
May 20 2014	RTK-DGPS	1-19
January 9 2015	RTK-DGPS	1-19

Figure 2.2: Location map showing the HMSC beach and shoreline monitoring network. Blue shaded dashed line denotes the cobble 'lag' toe of the original dynamic revetment, green shaded dashed line denotes the cobble 'lag' toe for the expanded section and grey shaded dashed line denotes the location of rip rap rock. Solid black line depicts the most recent (January 2015) measurement of the erosion scarp.

Figure 2.3 presents the change over time as measured at the 2.4 m elevation contour for all the transect sites that span the original dynamic revetment. Individual profile responses and time stacks (EDA plots) of changes taking place at selected contour elevations can be accessed online using the NANOOS Beaches portal: http://nvs.nanoos.org/BeachMapping. To view these data, select "Newport" in the regions section of the web portal. From there it is possible to obtain a close-up view of the HMSC campus and access the individual data plots.

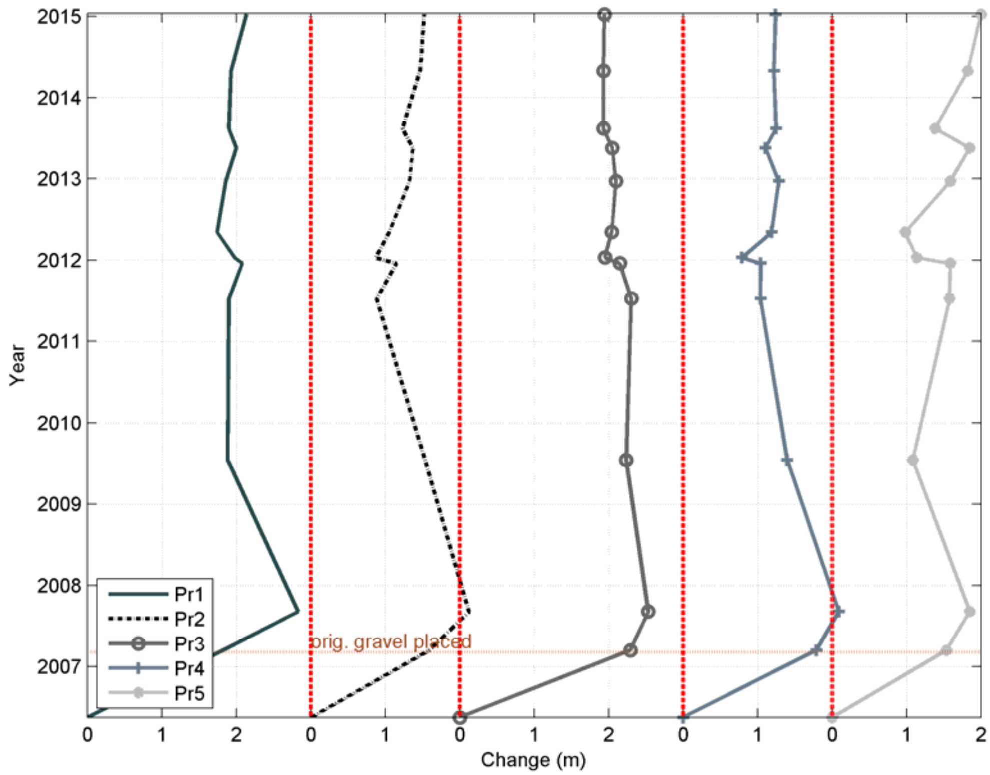

Figure 2.3: Transects 1 to 5 span the region where the original dynamic revetment/gravel beach was constructed. The zero line reflects the initial survey prior to construction of the gravel beach.

Figure 2.3 depicts the measured changes in the original gravel beach (Figure 2.4) area (blue dashed line in Figure 2.2). Examination of these data and results from the adjacent transects (6-12) confirm that the placement of gravel on the beach face and a lower cobble "lag" berm located at the juncture between the sandy beach and the inter-tidal mudflats, has been successful in stabilizing further retreat of the beach. This is characterized by the fact that there have been negligible changes to the gravel beach morphology in this area over time. Nevertheless, while the gravel beach is considered to be stable, there is some evidence of minor erosion taking place on the upper portion of the gravel beach where it merges with the sandy backshore. This response is entirely due to the occurrence of wind driven waves coupled with high tides, which enable the waves to reach to higher elevations on the profile (effectively exceeding the gravel beach) where they erode the sandy backshore. As noted in our original design, the gravel beach structure would need to have been built to a higher elevation to mitigate these effects, or combined with an artificial dune (*letter to HMSC by Allan, J.C. 2006*).

Figure 2.4: View looking northwest across the original gravel beach. Photo depicts the effects of periodic inundation due to high tides along with some minor erosion of the top of the sandy beach [Photo by J.C. Allan, January 9th 2015].

Further south between Transects 6-11 (Figure 2.5, green dashed line in Figure 2.2), the beach survey data indicate that the expanded gravel beach section is also considered to be stable, such that erosion of the beach and backshore has essentially ceased. Note that the degree of erosion that took place in this area is captured by the changes that took place between July 2009 and our first survey of the new gravel beach area undertaken in July 2011. In Figure 2.5 the baseline for our current monitoring efforts is the 2009 LIDAR. Despite the apparent stability of the gravel beach, our most recent survey undertaken on January 9th 2015 confirmed that the Transect 6 profile site is experiencing some erosion; this was noted in our previous report. As can be seen in Figure 2.6, the erosion is confined entirely to the upper part of the beach profile (located between the 2-3 m elevation). It is likely that the erosion at Transect 6 reflects the fact that this area of the beach may be feeding gravel to the areas adjacent to it (Figure 2.7). For example, Transect 5 shows clear evidence of it having gained gravel over the past few years. <u>As noted in our previous reports, we recommend that HMSC consider adding some additional gravel to this portion of the existing dynamic revetment in order to safe guard its volume</u>.

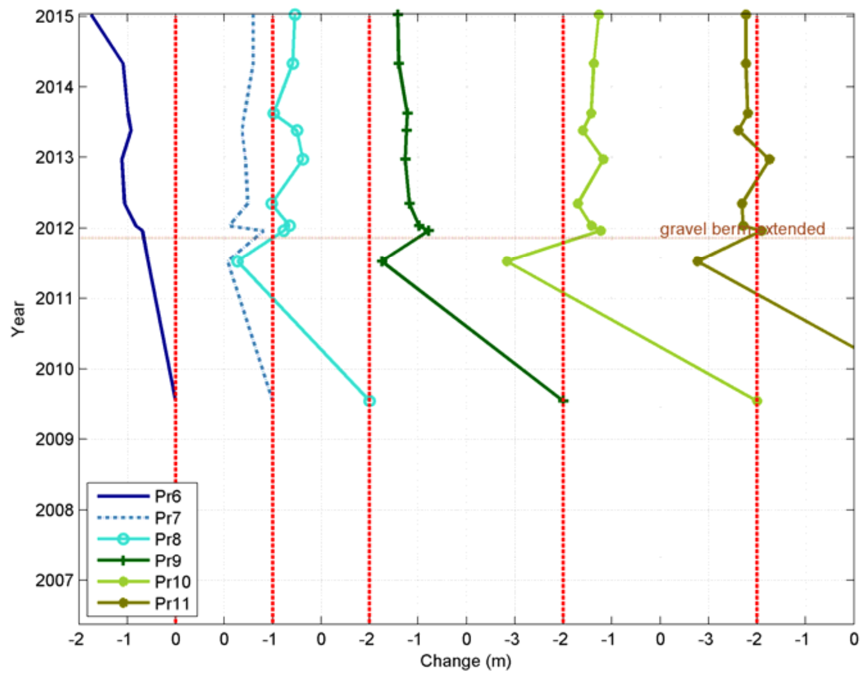

Figure 2.5: Transects 6 to 11 span the region where the expanded dynamic revetment/gravel beach was constructed. The zero line reflects the initial survey prior to construction of the gravel beach.

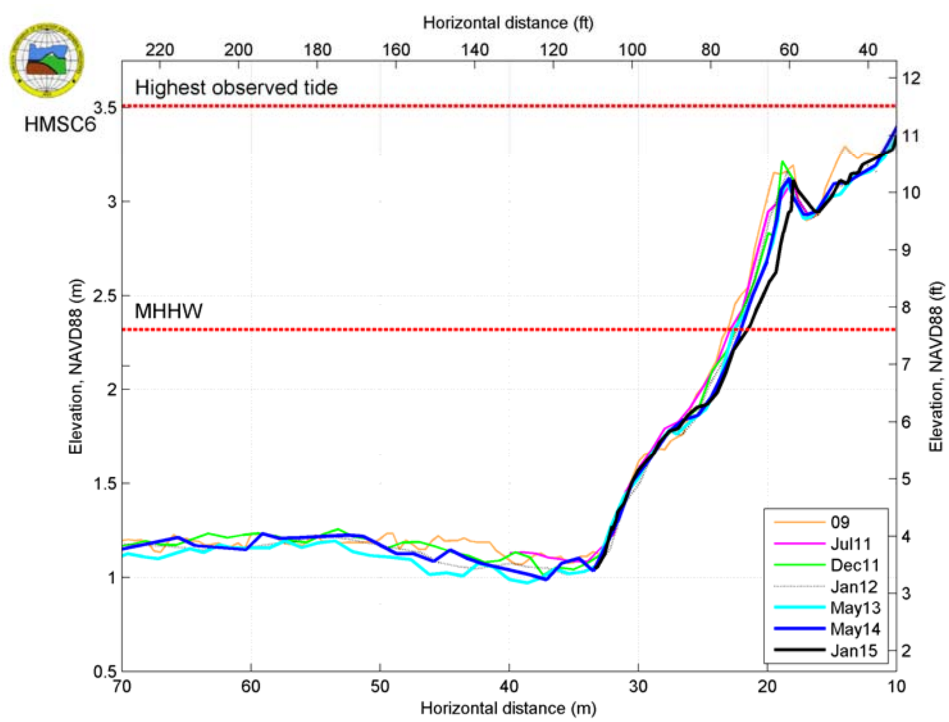

Figure 2.6: Measured profile changes at the Transect 6 profile site, showing evidence of erosion along the upper gravel beachface.

Figure 2.7: Erosion of the upper gravel beach and backshore occurring near the Transect 6 profile site [Photo by J.C. Allan, January 9th 2015].

Figure 2.8 depicts the measured changes taking place in the control area. As can be seen from the various plots, the southern "control" area continues to experience significant erosion, with some areas having eroded by 9.6 to 11 m (respectively HMSC 13 and 12), decreasing to -3.4 m at Transect 14 and -5 m at Transect 15. In each of these cases, the current rate of erosion is virtually unchanged between the period prior to and post gravel beach construction, which indicates that the erosion is independent of the recently constructed gravel beach. As noted in our earlier report, these changes reflect a complete landward translation of the entire beach profile (Figure 2.9). Hence, based on current patterns, we fully expect the erosion to continue to occur in the south. Figure 2.10 provides a current photo of the ongoing erosion of the control area, while the solid black line depicted in Figure 2.2 captures the spatial extent of the erosion along the length of the control area (and beyond). It is important to note that the erosion taking place adjacent to the south end of new gravel beach is entirely a function of antecedent erosion that is taking place along the entire length of this shore and is not related to any end effects associated with the expanded gravel beach. Accordingly, in the absence of the gravel beach the shoreline would almost certainly have removed the estuary trail located between Transects 7 to 11.

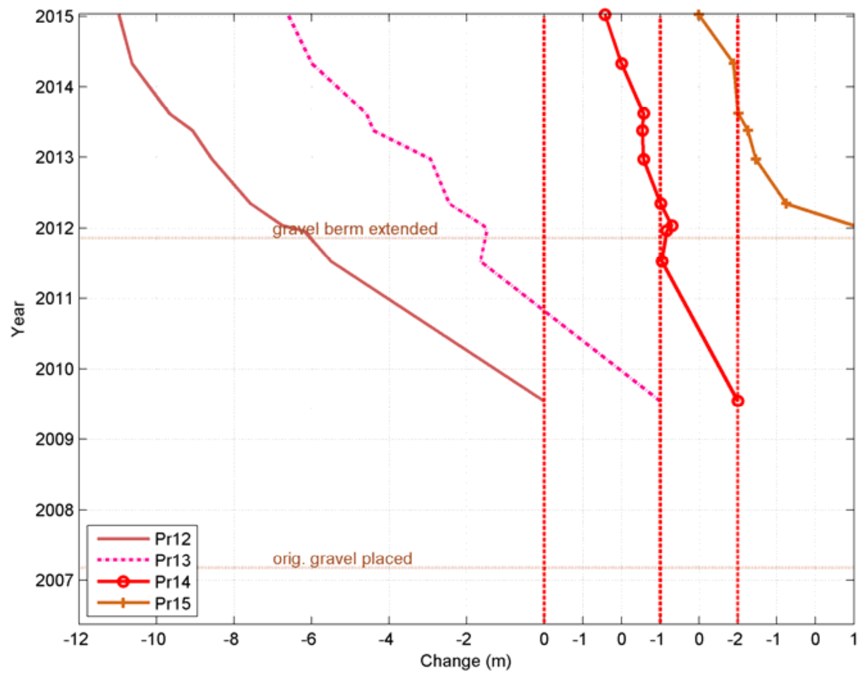

Figure 2.8: Transects 12 to 15 span the unprotected (control) region. The zero line reflects the initial survey prior to construction of the expanded gravel beach.

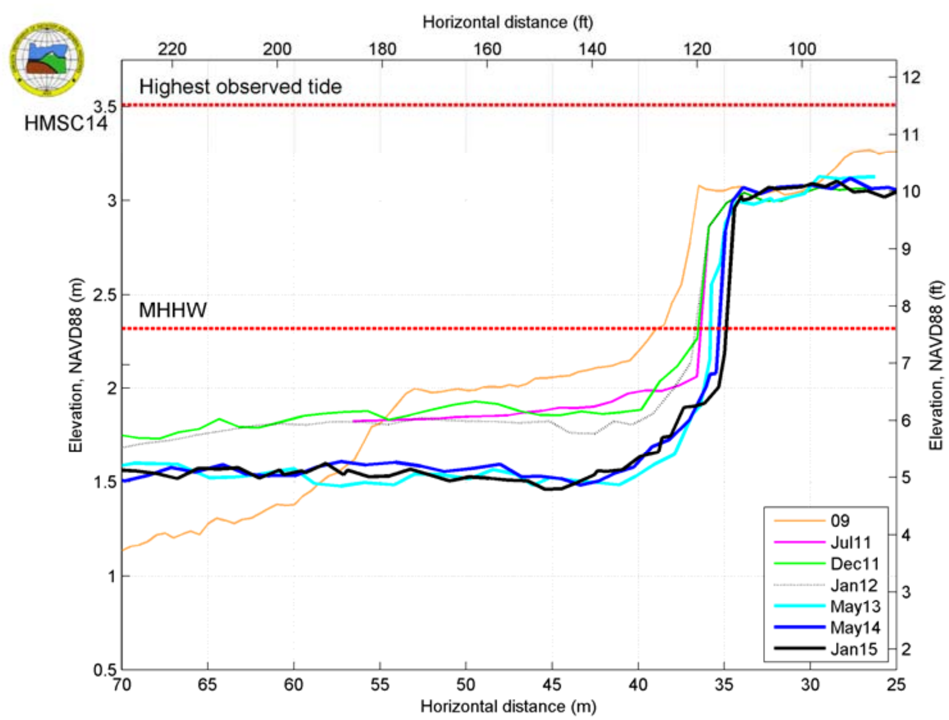

Figure 2.9: Measured profile changes at the Transect 14 profile site, showing the landward translation of the entire beach profile.

Figure 2.10: Recent erosion taking place in the control area [Photo by J.C. Allan, January 9th 2015].

2.3 References

Allan, J. C., and R. Hart (2008), Oregon beach and shoreline mapping and analysis program: 2007-2008 beach monitoring report. Rep. Open file report O-08-15, 60 pp, Oregon Department of Geology and Mineral Industries, Portland. <http://www.oregon.gov/ODOT/TD/TP_RES/docs/Reports/DynamicRevetments.pdf?ga=t>

Allan, J. C., R. Hart, and R. Geitgey (2005), Dynamic revetments for coastal erosion stabilization: A feasibility analysis for application on the Oregon Coast, Special Paper Rep. SP-037, 71 pp, Oregon Department of Geology and Mineral Industries, Portland, Oregon.

Komar, P. D., and J. C. Allan (2010), "Design with Nature" strategies for shore protection—The construction of a cobble berm and artificial dune in an Oregon State Park Rep., 117-126 pp, U.S. Geological Survey Scientific Investigations Report 2010-5254.

Nicholls, R., and N. Webber (1988), Characteristics of shingle beaches with reference to Christchurch Bay, S. England, paper presented at Proceedings of the 21st Conference on Coastal Engineering, ASCE.

Ruggiero, P., G. M. Kaminsky, G. Gelfenbaum, and B. Voight (2005), Seasonal to interannual morphodynamics along a high-energy dissipative littoral cell, Journal of Coastal Research, 21(3), 553-578.

Trimble (2011), Trimble R7 & R8 GPS system Manuals Rep., 106 pp, Trimble Navigation Limited, Dayton, Ohio.

van Hijum, E. (1974), Equilibrium profiles of coarse material under wave attack, paper presented at Proceedings 14th Conference on Coastal Engineering, ASCE

3.0 Biological Parameters

3.1 Density of Benthic Invertebrates

3.1.1 Benthic Invertebrate Sampling Methods

Mixed algae and seagrass samples were collected on October 3, 2014 from the wrack line deposited by the previous high tide at five random locations from the Reference beach, the DRP beach, and from the wrack line in the 2007 DRP area, termed DRP Reference. Figure 3.1 shows a typical algal wrack line along the DRP area. Samples of wrack were obtained by using scissors to cut segments of the wrack line which were rapidly placed in labeled plastic bags. Samples were placed in a walk in freezer until they could be thawed and sorted. The wrack samples consisted mostly of green macroalgae and the seagrass, *Zostera marina*. Wrack samples were processed by a combination of rinsing, sieving and picking the wrack material in plastic tubs. The algae/seagrass biomass material was saved for each replicate and dried in an oven at 70° C for 5 days. The final dry weight of each wrack sample was determined. Organisms were sorted, identified and counted. Densities for wrack associated organisms in higher taxonomic groupings are expressed per unit dry wrack biomass.

3.1.2 Invertebrate Results

Invertebrates associated with beach wrack were found within all three of the DRP study areas. Composition of wrack invertebrates was generally similar among the three areas. Invertebrate abundance was dominated (92%) by talitrid amphipod crustaceans (beach hoppers) (Table 3.1). A small number of juvenile mollusks (mussels, clams and snails), isopod crustaceans, insects, and oligochaetes that had settled on the algae prior to stranding were also found. Expressed as the number of individuals per g of plant dry-wt, there was a significant difference in density of wrack invertebrates among the three areas (One-way ANOVA, $p<0.002$). Pairwise multiple comparisons showed that the DRP area had significantly higher abundance per unit dry wt versus both the Reference and DRP Reference samples. Variability among samples was high, and for analysis of variance for simple abundance among sample areas for both total invertebrates and talitrid amphipods, normality tests failed. Kruskal-Wallis One Way ANOVA on Ranks was instead carried out, and no significant differences among sample areas was found for either parameter.

As in 2012 and 2013, deposition of wrack within the Reference area was inhibited due to the presence of vertical scarps along the shoreline resulting from the rapid erosion. Wrack was sparser and very patchy in the Reference area, compared to either of the other two beach areas sampled, where continuous wrack lines were present. Thus the total invertebrate abundance along the wrack line would have been much less in the reference area due to the limited quantities of wrack being accumulated.

Figure 3.1. View of the DRP shoreline (December 2014) showing algal wrack line on the upper shore. Note woody debris.

Table 3.1. Abundances (counts) of invertebrates collected in association with plant wrack deposited within the study area. DRP – 2011 project area, REF – Reference area, DRP REF – 2007 project area.

Sample	Amphipoda Talitridae	Isopoda	Mollusca	Oligo-chaeta	Insecta	Other	Total	#/g algae dry wt
DRP 1	2		1				3	4.58
DRP 2	8		2				10	8.73
DRP 3	3		2				5	8.45
DRP 4	7	1	1			1	10	7.12
DRP 5	27					1	28	7.87
Subtotal	**47**	**1**	**6**	**0**	**0**	**2**	**56**	
REF 1	35	2			2		39	0.49
REF 2	8		4		1	1	14	2.23
REF 3	26	6	1				33	4.52
REF 4		1					1	2.58
REF 5	1	3					4	3.47
Subtotal	**70**	**12**	**5**	**0**	**3**	**1**	**91**	
DRP REF 1	37				1		38	3.77
DRP REF 2	17	1	1				19	6.70
DRP REF 3	245		1	1			247	4.51
DRP REF 4	1		1		1		3	5.17
DRP REF 5	1						1	2.42
Subtotal	**301**	**1**	**3**	**1**	**2**	**0**	**308**	

3.2 Fish

3.2.1 Fish Sampling Methods

From January through November of 2014, intertidal fish were captured with a 50-ft (15.3 m) shore seine towed perpendicularly to the shore for a distance of 50 ft (15.3 m) at three permanent sampling sites along the DRP shoreline and three permanent sites along the Reference shoreline (Figure 3.6). This sampling was performed once per month at spring high tide in order to sample as much of the high intertidal habitat as possible. All fish captured in the seine were held for no more than 15 minutes in a container of ambient bay water while they were measured and identified to the lowest possible taxonomic level before being released at the point of capture.

3.2.2 Fish Results

During eleven months of sampling, a total of 12 species and 2794 individuals were captured (Table 3.2, Figure 3.2). Eight species were represented by 10 or fewer individuals in the total collection (Table 3.2). During the 2014 sampling year, 424 individuals representing 9 species were captured along the DRP shoreline (sites 1-3) and 2370 individuals representing 9 taxa were collected from the reference shoreline (sites 4-6) (Figure 3.3). Chum salmon fry, first collected in 2013, were again present, with 202 individuals captured predominantly in the month of April that were evenly distributed between the two shorelines (Figure 3.4). One juvenile Chinook salmon was captured on the DRP shoreline during that month as well. Approximately 85% of the total number of individuals captured in 2014 was collected from the reference shoreline sites (Figure 3.3), a figure comparable to that from 2013 (80%). That proportion was driven primarily by a large catch of whitebait smelt in February (Figure 3.2) at site 6 of the Reference shoreline (Figure 3.2). As in previous years, Pacific Staghorn Sculpin, Whitebait Smelt, and Shiner Perch were the 3 most abundant fishes captured (Table 3.2). The largest differences as compared to 2013 were the far lower number of Dungeness crab and the far higher number of Chum Salmon collected. Statistical comparisons indicated that there was a significant difference between two shoreline areas in mean abundance, no significant difference among dates, and that there was no significant interaction term of shoreline with date (Two-way ANOVA). Mean monthly catch was significantly greater in the reference shoreline area than the catch in the DRP shoreline area ($p = 0.028$).

Table 3.2. A list of the total number of individuals of each species captured in 2014, during eleven months of sampling both the DRP and the Reference shoreline sites.

Species	Common Name	Total
Leptocottus armatus	Pacific Staghorn Sculpin	1293
Allosmerus elongatus	Whitebait Smelt	1049
Cymatogaster aggregata	Shiner Perch	213
Oncorhynchus keta	Chum Salmon	202
Oligocottus snyderi	Fluffy Sculpin	10
Gasterosteus aculeatus	Three-Spine Stickleback	8
Hemigrapsus oregonensis	Shore Crab	5
Unidentified Juvenile Fish		5
Hypomesus pretiosus	Surf Smelt	4
Platichthys stellatus	Starry Flounder	3
Oncorhynchus tshawytscha	Chinook Salmon juv	1
Metacarcinus magister	Dungeness Crab juv.	1
Grand Total		2794

3.2.3 Discussion

The results from the third year of post installation fish sampling were consistent with past results, in that more intertidal fish were captured along the Reference shoreline than the DRP shoreline. The interpretation of the reasons behind this difference may be influenced by multiple factors which are difficult to distinguish among. First, the seine net is most efficient on sandy, unobstructed bottom such as the reference area. While sampling the DRP shoreline, the seine net could not closely follow the contours of all sections of the bottom because of the prominent slope change where the cobble meets the sand at the base of the revetment. This may have provided fish an escape under the net that was not present while sampling the sandy bottom of the reference shoreline. Thus, a portion of the intertidal fish population in the DRP sites may be missed as a result of this gear limitation. Secondly, we have observed demersal fish seeking refuge from the seine net in the interstitial spaces between the cobble stones of the revetment during our sampling. These refugia are not present in the sandy habitat of the reference shoreline, which may also explain the larger catch of intertidal fish at those sites. Third, the systematic, sequential sampling of sites 1-6 may displace pelagic fish into subsequent sampling sites. It is possible that fish may be captured in larger numbers within the reference shoreline as a result of this directional displacement. Finally, the structural complexity along the reference shoreline is much higher due to the presence of exposed root wads of two trees, and several bushed which have collapsed to the intertidal. For these four reasons, the data collected may include bias in the comparison between areas.

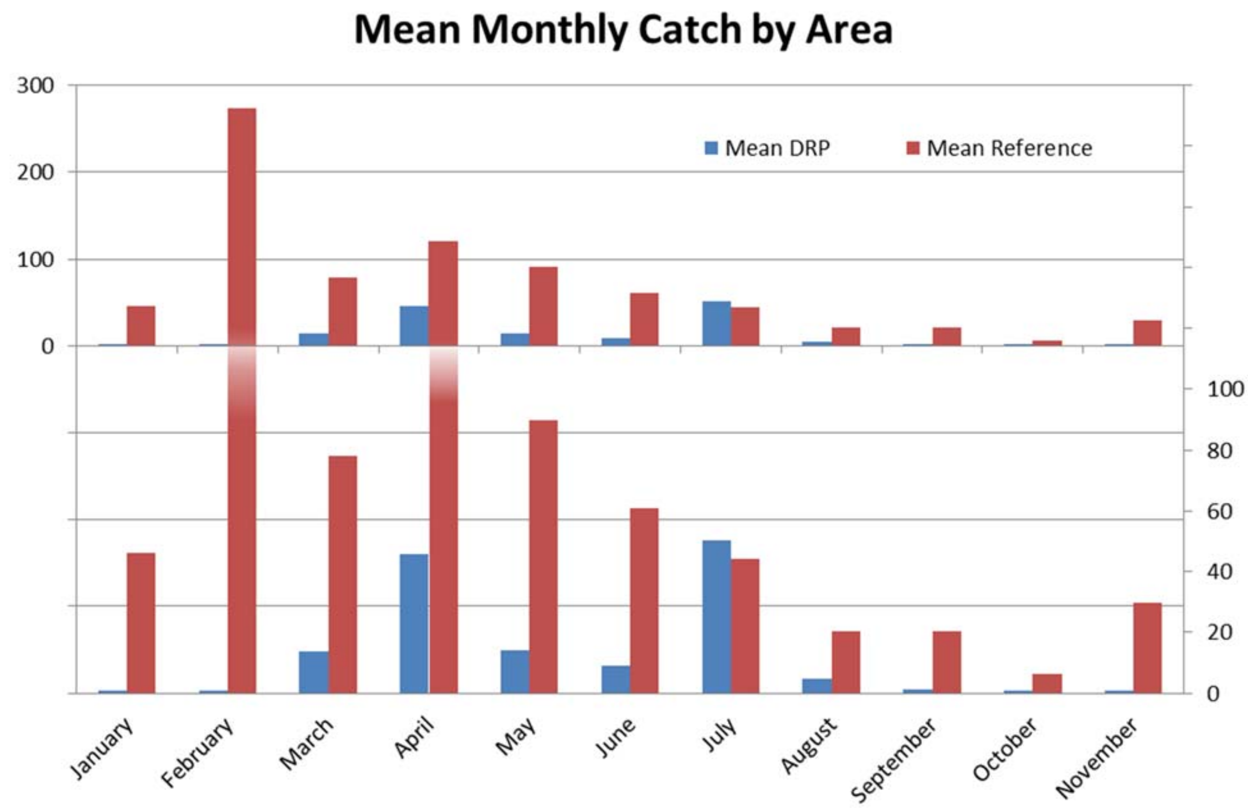

Figure 3.2: Top panel: Total number of individuals captured in both the DRP shoreline sites and the Reference shoreline sites during 2014. Bottom panel: The same data plotted on an expanded scale to focus on lower abundance sites.

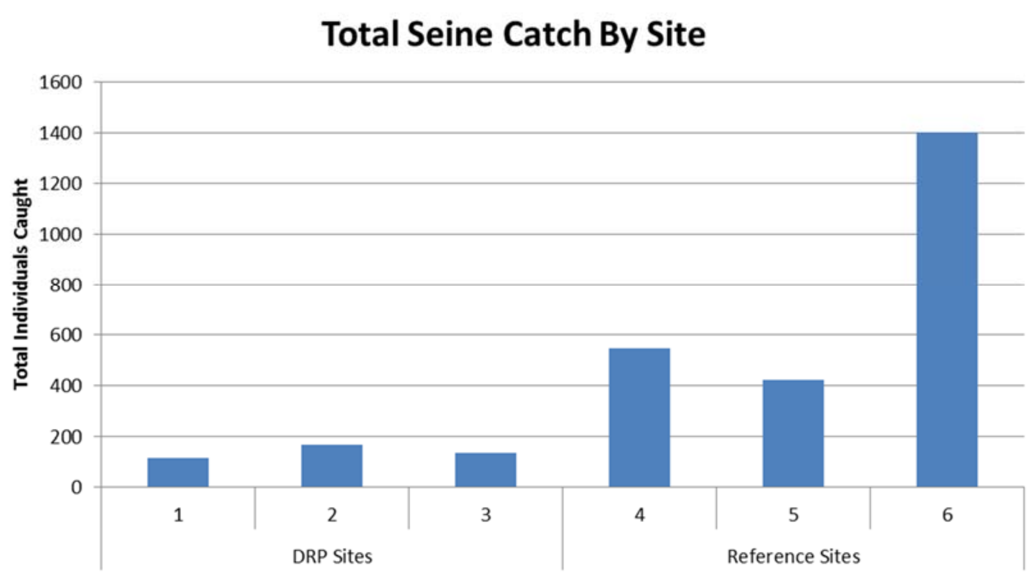

Figure 3.3: Total number of individuals caught at each sampling site in 2014. Sites 1-3 are within the DRP shoreline, sites 4-6 are in the Reference shoreline.

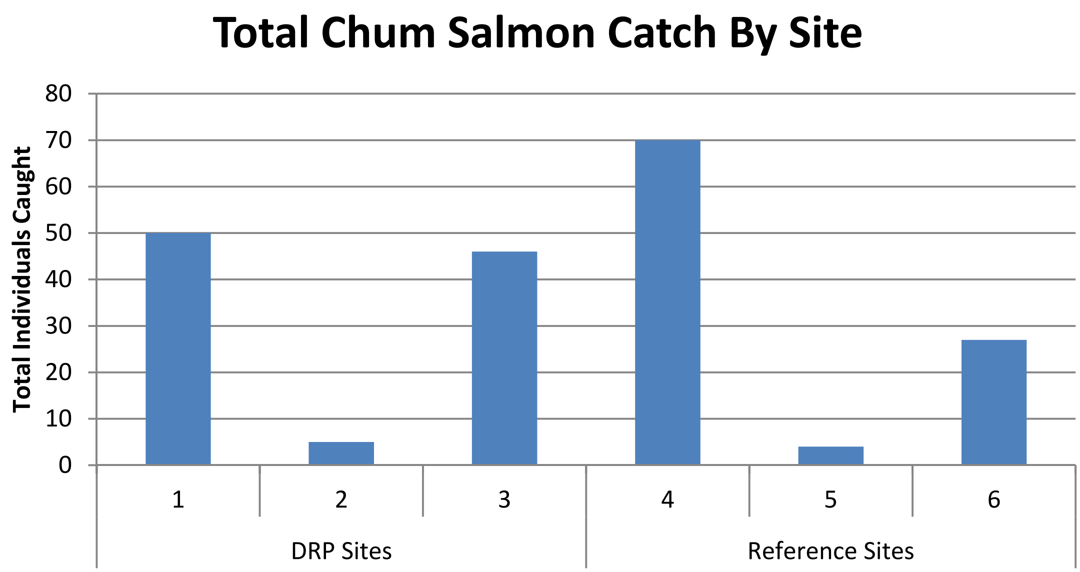

Figure 3.4: Total number of chum salmon fry individuals caught at each sampling site in 2014. Sites 1-3 are within the DRP shoreline, sites 4-6 are in the Reference shoreline.

In an attempt to validate the seine data, GoPro® cameras were mounted on poles and submerged in the intertidal waters off the revetment and reference shorelines for 40-60 minutes the day before each monthly seine sampling from May through November. A quantitative analysis of recorded video has not been completed at the time of this report. In preliminary video analysis, the number of fish sightings off the revetment is significantly greater than those off the reference area. The number of fish sightings in the revetment videos are difficult to quantify as the fish swim in and out of view repeatedly making it challenging to discern if there are many fish or repeated sightings of the same few fish. However, this implies the fish are either plentiful on the revetment or demonstrating habitat usage and not just transient presence. Regardless, the video recordings do not appear to be a successful approach to validating the seining abundances.

3.3 Vegetation

3.3.1 Vegetation Methods

To assess possible changes in shoreline vegetation following DRP installation, sampling was initially focused on the approximately 1 to 10 m wide strip of land between the paved HMSC estuary trail and the shoreline. This area contains mixed vegetation community types including high marsh, dune and terrestrial plants and shrubs. Six 1-m^2 quadrats were established within the DRP and Reference areas in October 2011 (Figure 3.5) and a labeled PVC stake was placed to mark the quadrat center. A Trimble R8 GNSS unit was used to establish horizontal and vertical positions of the center of each plot by performing an RTK survey with the ORGN network. Over the monitoring period to date, sample quadrats Reference 1, 2 and 3 have been lost to erosion. Quadrat 5 was partially eroded at the time of the 2014 vegetation sampling and plant data were excluded for this quadrat. A replacement quadrat was established for future sampling. Quadrat Reference 4 may also disappear within the next year and may require replacement. The new quadrats established inland of the original plots were designated as quadrats 1A, 2A, and 3A. Differences in plots due to relocation were discussed in the 2014 Monitoring Report.

Vascular plant presence or absence (usually at the species level) was visually assessed by scanning one 0.25 -m^2 quadrat within each 1-m^2 quadrat (Figure 3.6, 3.7). Plant percent cover was assessed by visually evaluating the percentage that each plant species contributed to the overall plant community present within the 1-m^2 quadrat. Percent cover estimates also considered non-plant substrata such as open or bare ground and detrital material. Photographs of each quadrat were taken from several perspectives.

3.3.2 Vegetation Results

All the plant taxa recorded in the 0.25-m^2 quadrats (Table 3.3) were also all recorded in the 1-m^2 quadrats. Based on the 1 m^2 quadrats, a total of twenty-six plant taxa were identified in the 11 plots (Table 3.4): 25 vascular plant taxa and 1 moss. Eight plant taxa were found in both areas, nine taxa were only observed within the DRP area, and ten were only observed within the Reference area. Within the 0.25-m^2 quadrats, a grass, *Festuca rubra* (red fescue), was the most frequently occurring taxon in the DRP, while sweet vernal grass (*Anthoxanthum odoratum*) was the most frequently occurring species in quadrats in the Reference area.

Estimates of percent coverage of plants gave generally similar results to those obtained from the presence-absence data (Table 3.4). There was a significantly higher coverage of living plant material, and conversely a greater percentage of non-living coverage in the Reference area, which was the same result observed in the sampling in 2013. The grass *F. rubra* had the largest percent coverage in the DRP. *Spergularia* spp. (sea-spurreys, sandspurrys) and *Elymus mollis* (American dunegrass) were the next most abundant in terms of percent cover in the DRP. *Carex pansa* (sand dune sedge), *Ammophila arenaria* (European beachgrass), and *Juncus breweri* (Brewer's rush) were the most extensive in the Reference area quadrats. Dominant species were generally similar to the 2014 survey in the DRP plots, with the top three species in percent area being the same. In the Reference quadrats, the relative representation of *Carex pansa* increased, and that of *Juncus breweri* decreased, as compared to values measured in 2013.

The lower average vegetation cover at the DRP sites has been a consistent result during the monitoring, and was present in the pre-project samples. DRP quadrats 1-3 occur at lower elevation than most other sample locations, and as described in previous reports, there is also a topographic low spot in the shoreline near beach profile 9 (Figure 3.1), which allows the back shore area to be more frequently flooded by fall and winter King tides.

Figure 3.5: Vegetation plots in DRP (red symbols, DRP 1-6) and Reference (yellow symbols, Ref 1-6) survey areas. Locations of fish sampling transects are shown as green (DRP, Fish 1-3) and orange (Reference, Fish 4-6) symbols.

Figure 3.6: Close up of 1-m^2 quadrat used to determine plant presence-absence with the 0.25-m^2 quadrat used to determine percentage cover of vegetation, October 2014.

Figure 3.7: Vegetation monitoring Quadrat DRP 1, October 2014. View to northeast.

Table 3.3. Frequency of occurrence (presence/absence) of plant taxa in the DRP and Reference areas, n = 6 (0.25-m^2) quadrats for DRP and n=5 for Reference.

Plant Taxon	DRP	Reference
Festuca rubra	5	2
Grindelia stricta	3	1
Taraxacum sp.	3	1
Daucus carota	3	0
Moss (unknown sp.)	2	1
Atriplex spp.	2	1
Spergularia spp.	2	0
Elymus mollis	2	0
Rumex acetocella	2	0
Anthoxanthum odoratum	1	3
Angelica lucida	1	1
Schedonorus phoenix	1	0
Stellaria spp.	1	0
Digitalis purpurea	1	0
Cytisus scoparius	1	0
Carex pansa	0	2
Juncus breweri	0	2
Carex obnupta	0	1
Deschampsia cespitosa	0	1
Jaumea carnosa	0	1
Sarcocornia perennis	0	1
Ammophila arenaria	0	1
Erechtites minima	0	1
Rubus spp.	0	1

Table 3.4. Mean percent coverage of plant taxa and non-living material in the DRP and Reference areas, n = 6 (1-m^2) quadrats for DRP and n=5 quadrats for Reference.

Plant Taxon	DRP	Reference
Festuca rubra	26.7	0.2
Spergularia spp.	10.8	0.0
Elymus mollis	10.2	0.0
Schedonorus phoenix	8.2	0.0
Atriplex spp.	5.8	0.0
Rumex acetocella	3.0	0.4
Taraxacum sp.	3.0	0.2
Moss (unknown sp.)	2.5	0.8
Grindelia stricta	2.2	0.0
Anthoxanthum odoratum	1.0	2.2
Digitalis purpurea	1.0	0.2
*Daucus carot*a	1.0	0.0
Unknown weed	0.8	0.0
Angelica lucida	0.5	3.0
Stellaria spp.	0.3	0.0
Cytisus scoparius	0.2	0.0
Carex pansa	0.0	33.8
Ammophila arenaria	0.0	14.2
Juncus breweri	0.0	11.2
Jaumea carnosa	0.0	7.0
Sarcocornia perennis	0.0	6.0
Deschampsia cespitosa	0.0	5.0
Carex obnupta	0.0	3.0
Rubus spp.	0.0	1.2
Distichlis spicata	0.0	1.0
Erechtites minima	0.0	0.2
Total Non-living		
Bare ground/sand	9.5	1.2
Dead plant matter	9.2	6.2
Woody Debris	4.2	3.0

4.0 Current Status of Erosion in the Study Area

As described in more technical detail in Section 2.2, as of February, 2015, both the 2007 and 2011 DRP shoreline sections appear mostly stable, while erosion has continued to occur in the Reference area immediately to the south of the DRP. "King" tides occurring from November – February coupled with east wind driven wave action have continued to roll back the shoreline vegetation, and steep vertical scarps at the vegetation edge are the norm along this shore section. Erosion in the unprotected Reference area in the period 2009-2014 has been as great as 11 m (36 ft). The effect of erosion during 2014 can be seen in comparison of Figures 4.1 through 4.4, taken from a similar spot on the HMSC Nature Trail. Erosion in 2014 continued to create vertical banks of collapsed sod, with salt march vegetation collapsing and being eroded away (Compare Figures 4.5 and 4.6). Erosion has begun to accelerate for low salt marsh habitat beyond the southern edge of the currently proposed new project area, which has not been exposed to erosion before (Figure 4.7).

Figure 4.1: View of collapsed section of HMSC nature trail, February 3, 2012.

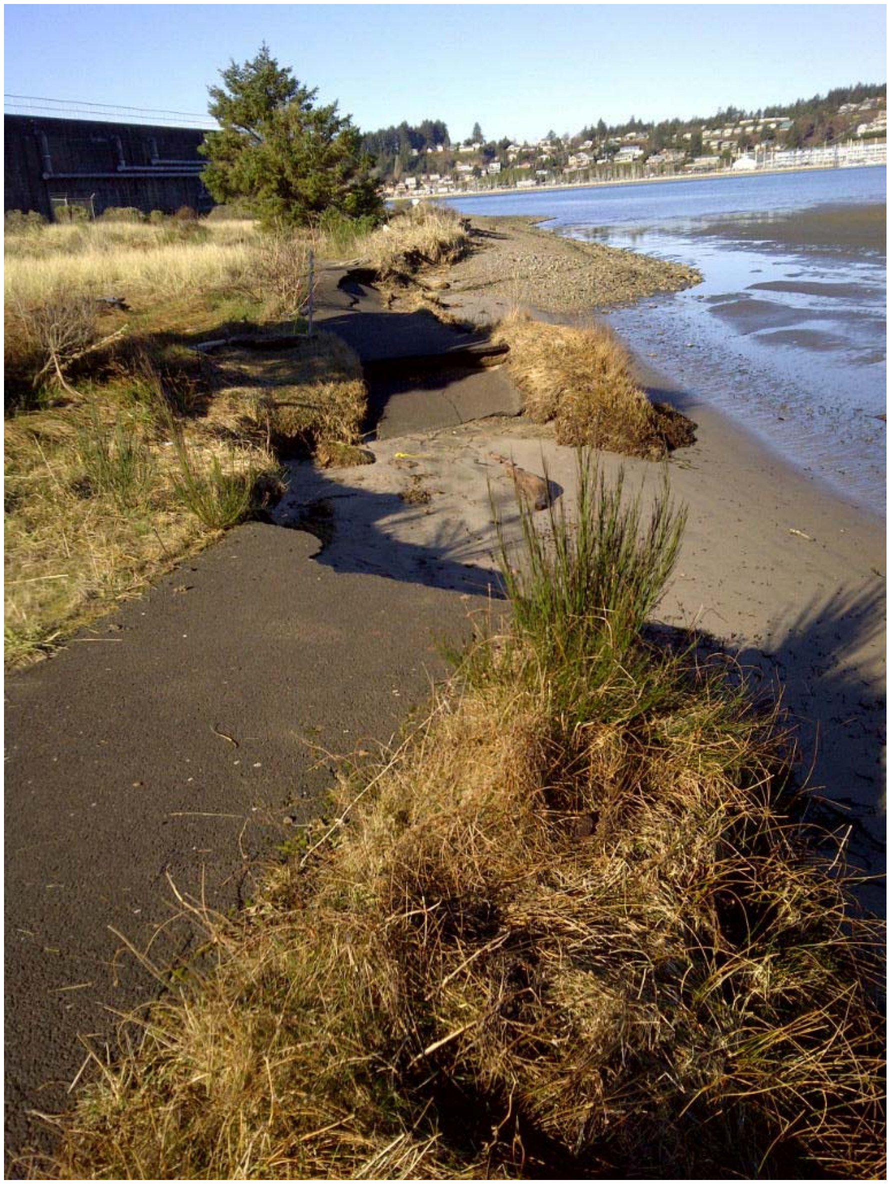

Figure 4.2: View of eroded section of HMSC nature trail, January 16, 2013.

Figure 4.3: View of eroded section of HMSC nature trail, February 14, 2014. The terminus of the 2011 dynamic revetment is seen in the upper center of the photo, and the offset caused by shoreline erosion is clearly visible.

Figure 4.4: View of eroded section of HMSC nature trail, January 26, 2015. Erosion has continued unabated landward of the original position of the asphalt nature trail. Several floating docks broke loose during storms and stranded on this section of shore.

Figure 4.5: View to the south of the 2011 DRP in the Reference area (February 14, 2013), showing collapsed banks with 4 foot vertical scarps. In the upper left, erosion is now starting to attack low salt marsh habitat on the point and beyond which has not previously been exposed to erosion.

Figure 4.6: View to the north in the Reference area (January 26, 2013), showing collapsed banks with vertical scarps and additional section of collapsed asphalt due to continued rapid erosion.

Figure 4.7: Erosion is now starting to attach low salt marsh habitat beyond the area which previously been exposed to erosion. Note presence of vertical scarping.

5.0 Disclaimer

The information in this document contained in sections 3.1 and 3.3 has been subjected to review by the National Health and Environmental Effects Research Laboratory of US EPA and approved for publication. Approval does not signify that the contents reflect the views of the Agency, nor does mention of trade names or commercial products constitute endorsement or recommendation for use.

Appendix 1: Beach Profile Survey Graphs

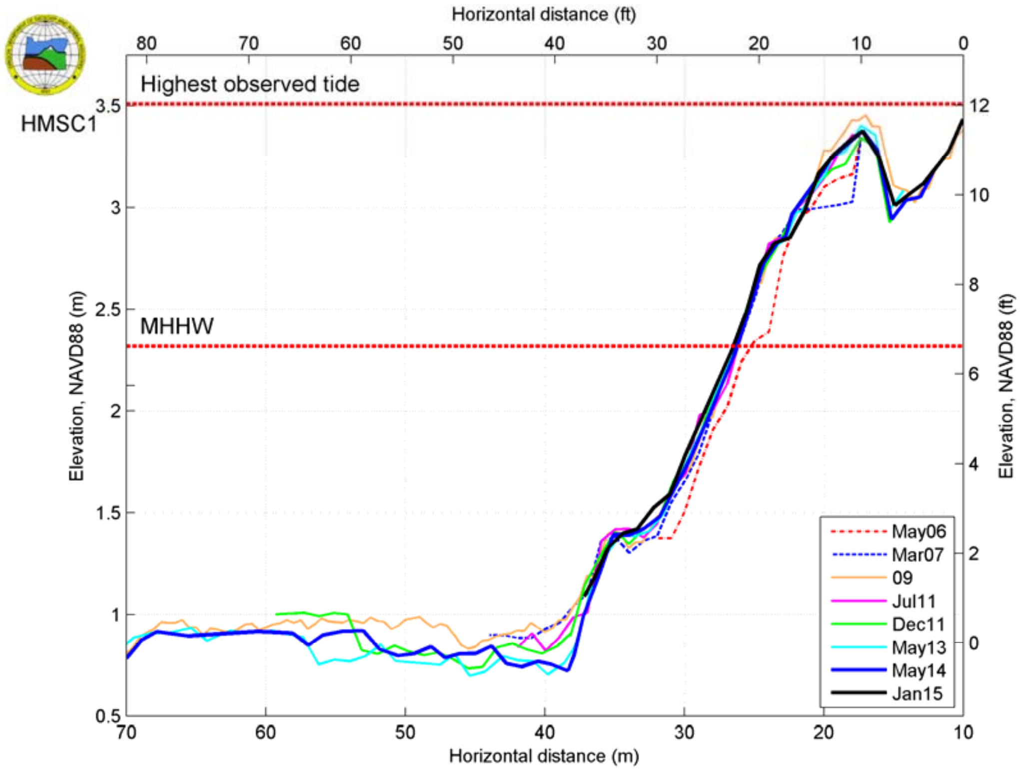

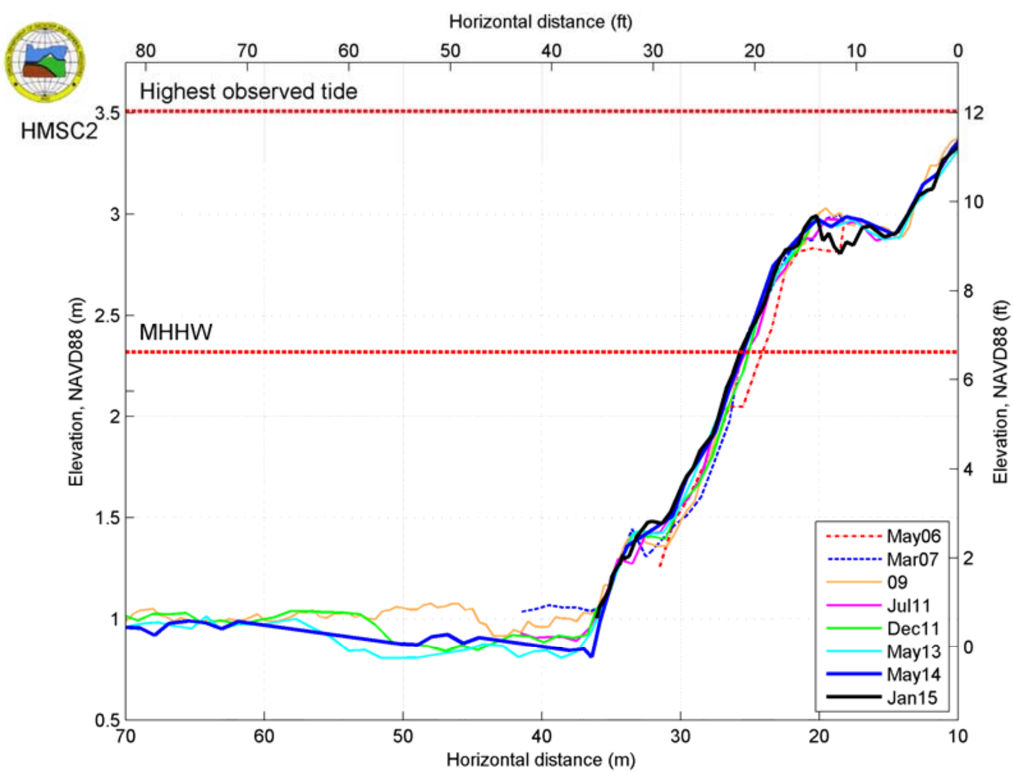

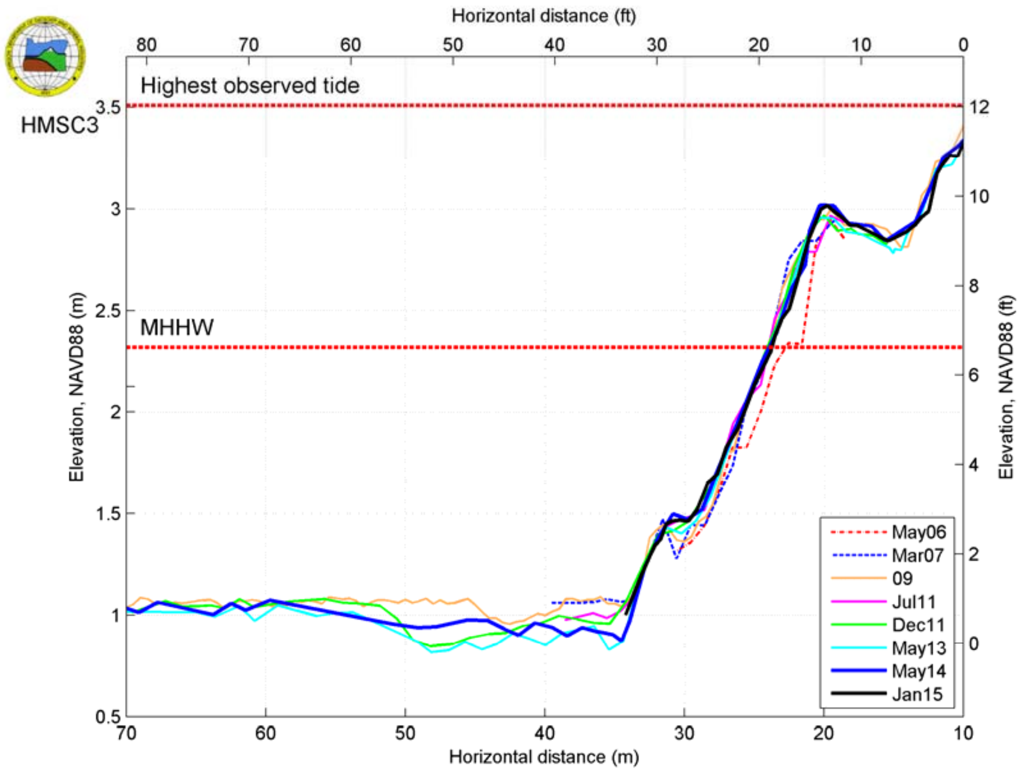

Horizontal distance (ft)
80
70
60
50
40
30
20
10
0
Highest observed tide
HMSC3
3.5
3
2.5
2
1.5
1
0.5
Elevation, NAVD88 (m)
MHHW
12
10
8
6
4
2
0
Elevation, NAVD88 (ft)
May06
Mar07
09
Jul11
Dec11
May13
May14
Jan15
70
60
50
40
30
20
10
Horizontal distance (m)

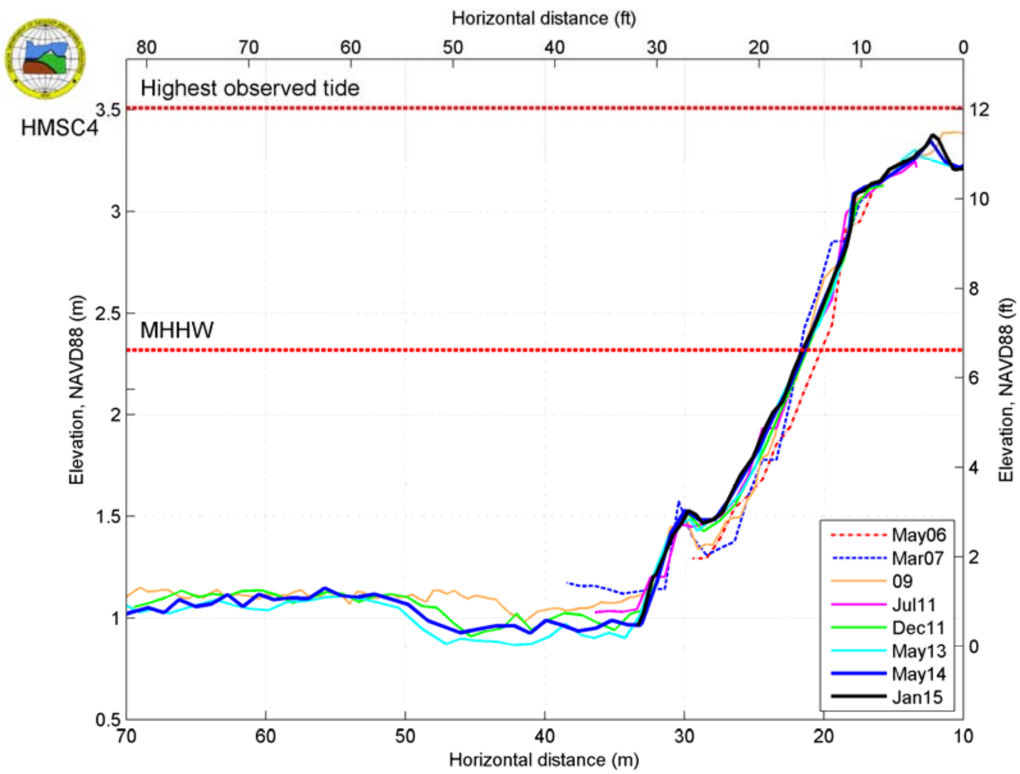

Horizontal distance (ft)
80
70
60
50
40
30
20
10
0
Highest observed tide
HMSC4
3.5
3
2.5
2
1.5
1
0.5
Elevation, NAVD88 (m)
MHHW
12
10
8
6
4
2
0
Elevation, NAVD88 (ft)
May06
Mar07
09
Jul11
Dec11
May13
May14
Jan15
70
60
50
40
30
20
10
Horizontal distance (m)

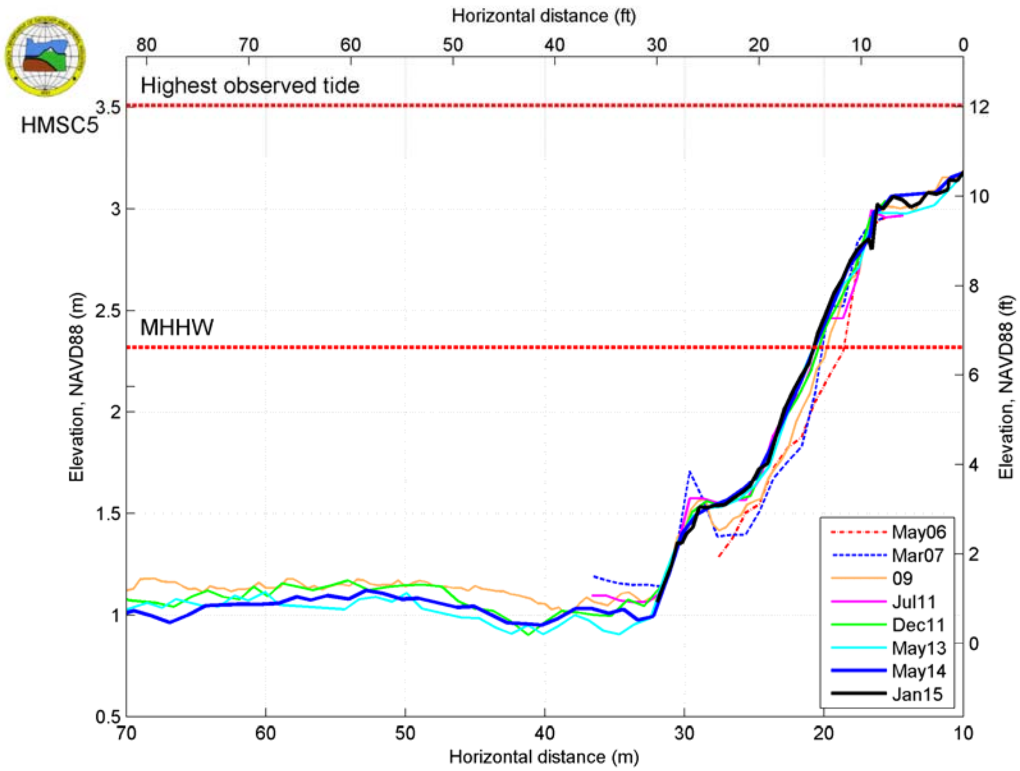
Horizontal distance (ft)
Highest observed tide
HMSC5
MHHW
Elevation, NAVD88 (m)
Elevation, NAVD88 (ft)
May06
Mar07
09
Jul11
Dec11
May13
May14
Jan15
Horizontal distance (m)

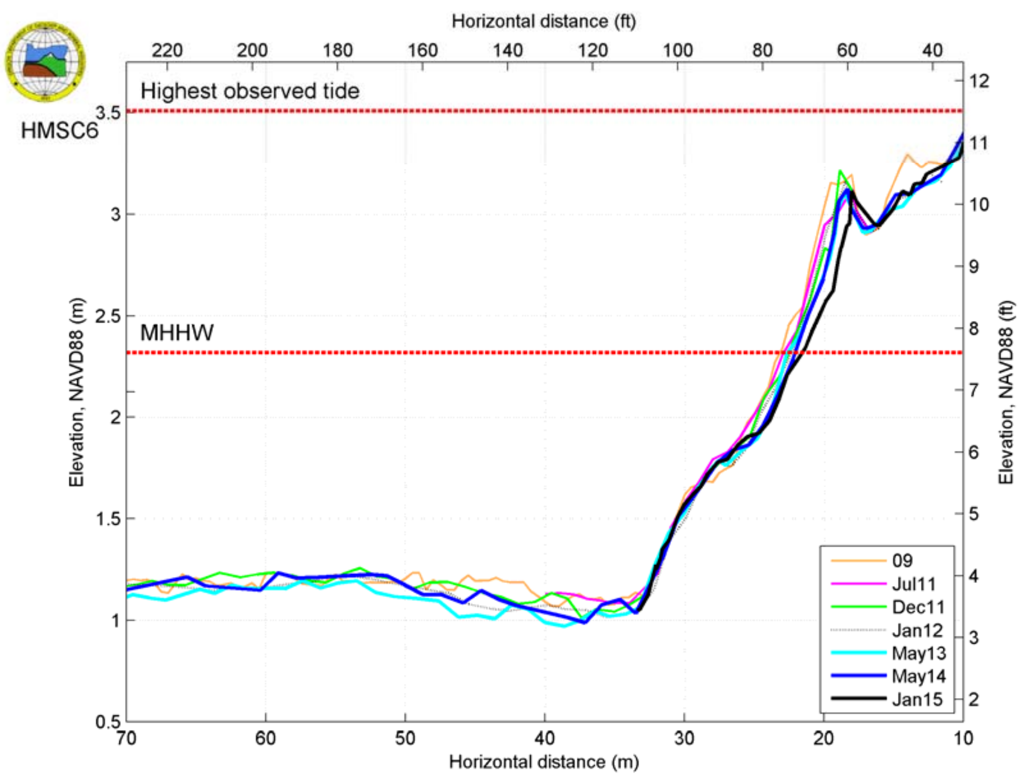
Horizontal distance (ft)
Highest observed tide
HMSC6
MHHW
Elevation, NAVD88 (m)
Elevation, NAVD88 (ft)
09
Jul11
Dec11
Jan12
May13
May14
Jan15
Horizontal distance (m)

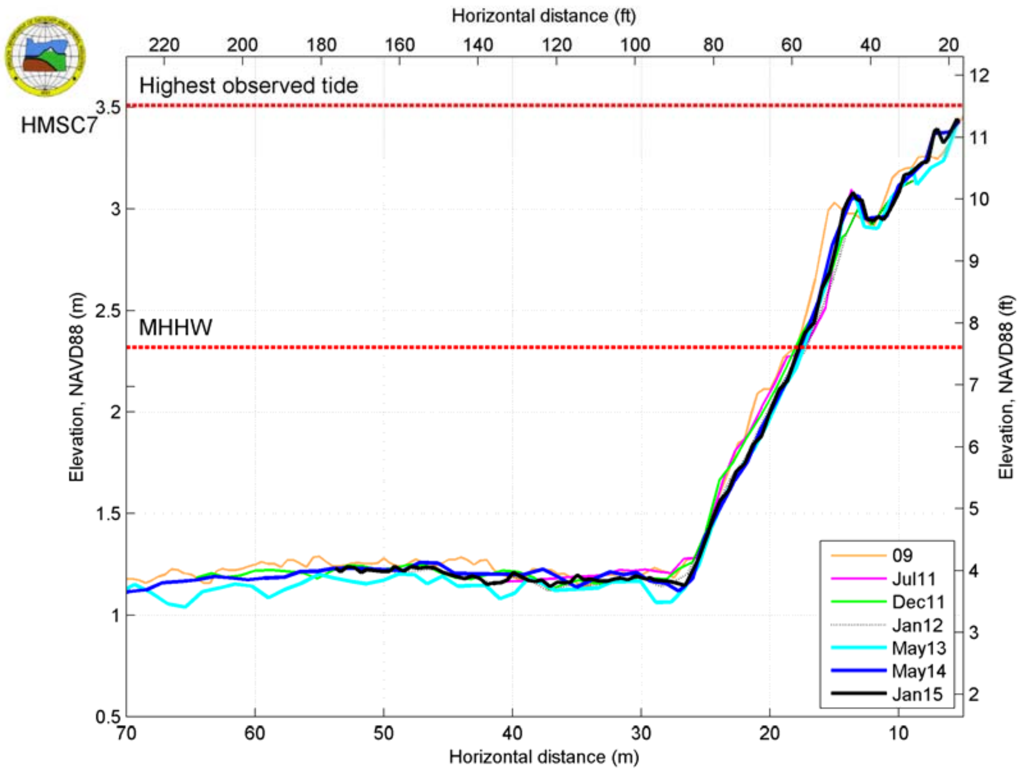
HMSC7
Horizontal distance (ft)
Highest observed tide
MHHW
Elevation, NAVD88 (m)
Elevation, NAVD88 (ft)
Horizontal distance (m)
09
Jul11
Dec11
Jan12
May13
May14
Jan15

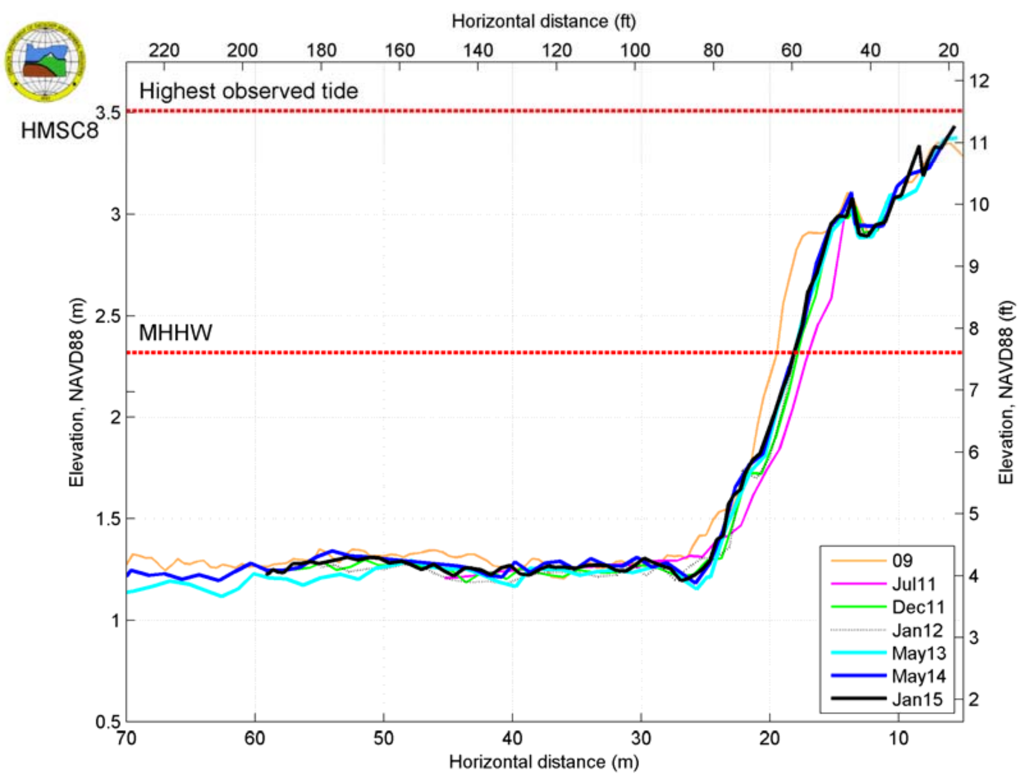
HMSC8
Horizontal distance (ft)
Highest observed tide
MHHW
Elevation, NAVD88 (m)
Elevation, NAVD88 (ft)
Horizontal distance (m)
09
Jul11
Dec11
Jan12
May13
May14
Jan15

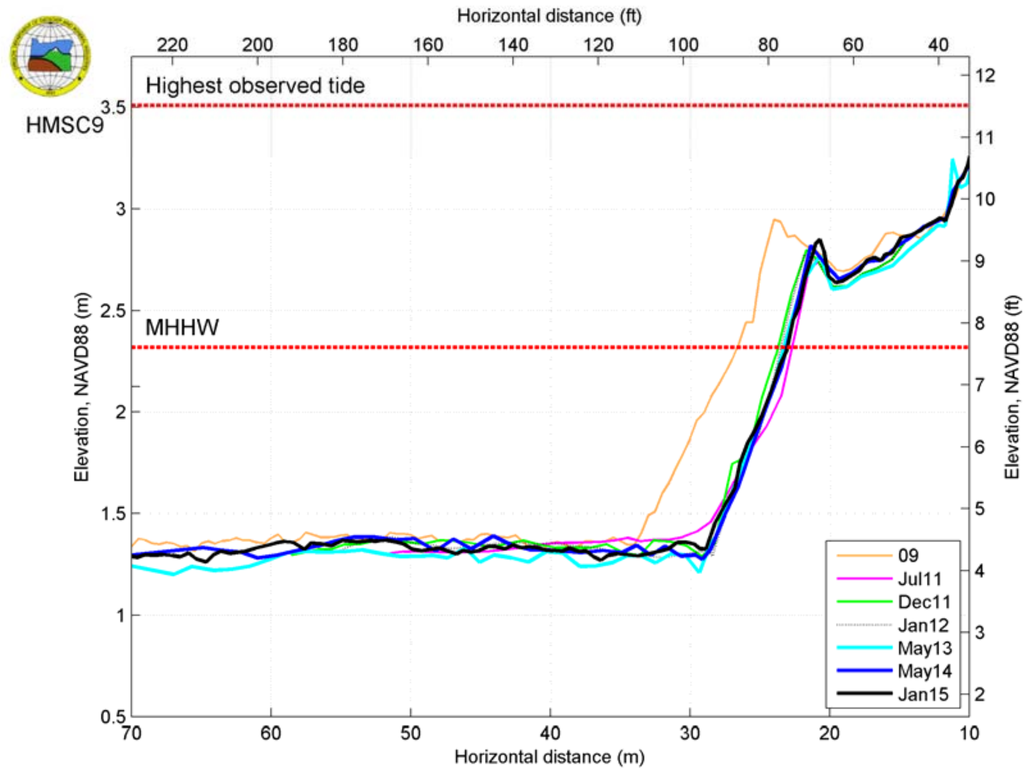
HMSC9
Horizontal distance (ft)
220
200
180
160
140
120
100
80
60
40
Highest observed tide
MHHW
Elevation, NAVD88 (m)
3.5
3
2.5
2
1.5
1
0.5
Elevation, NAVD88 (ft)
12
11
10
9
8
7
6
5
4
3
2
70
60
50
40
30
20
10
Horizontal distance (m)
09
Jul11
Dec11
Jan12
May13
May14
Jan15

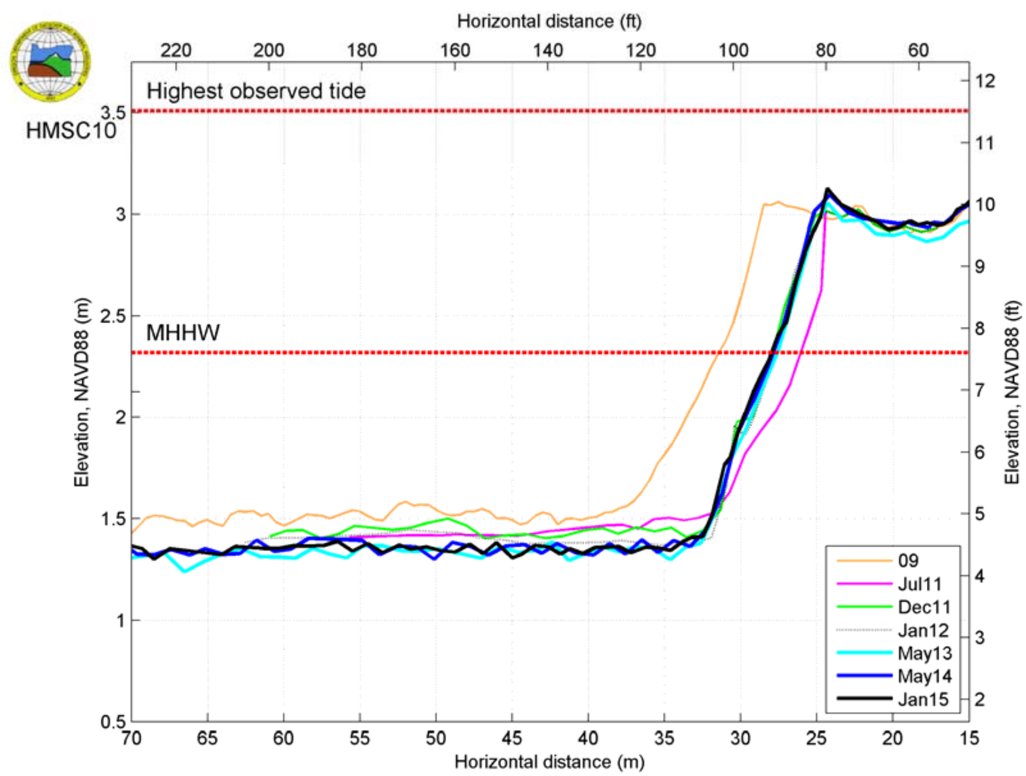
HMSC10
Horizontal distance (ft)
220
200
180
160
140
120
100
80
60
Highest observed tide
MHHW
Elevation, NAVD88 (m)
3.5
3
2.5
2
1.5
1
0.5
Elevation, NAVD88 (ft)
12
11
10
9
8
7
6
5
4
3
2
70
65
60
55
50
45
40
35
30
25
20
15
Horizontal distance (m)
09
Jul11
Dec11
Jan12
May13
May14
Jan15

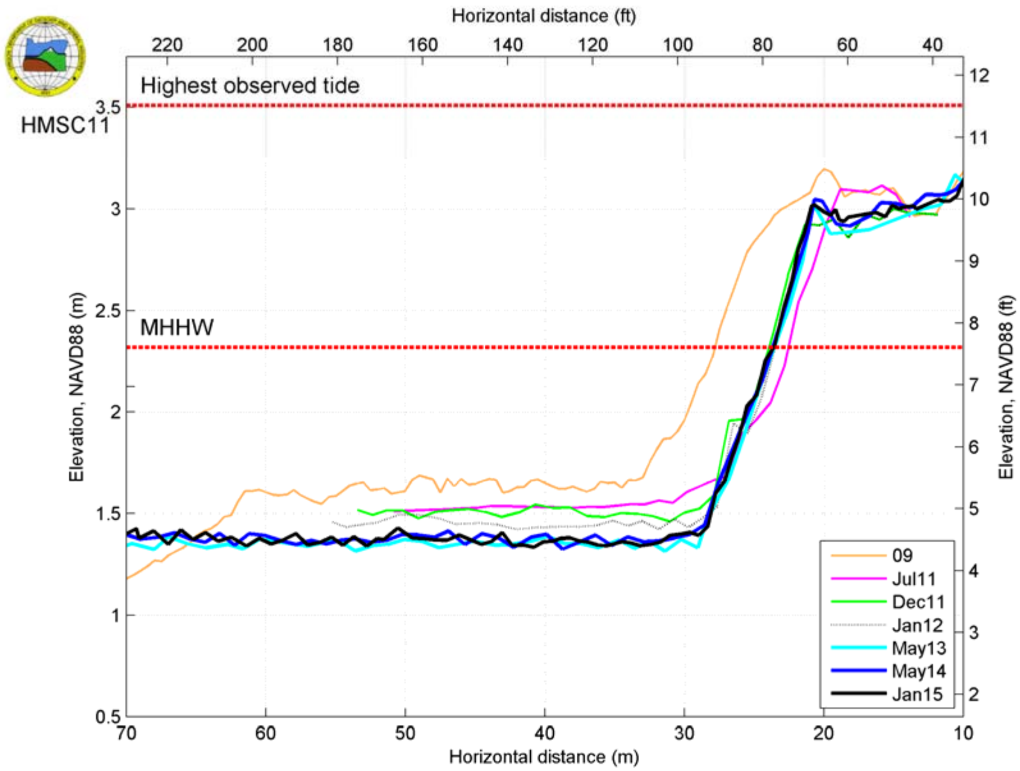

HMSC11
Horizontal distance (ft)
Highest observed tide
MHHW
Elevation, NAVD88 (m)
Elevation, NAVD88 (ft)
Horizontal distance (m)
09
Jul11
Dec11
Jan12
May13
May14
Jan15

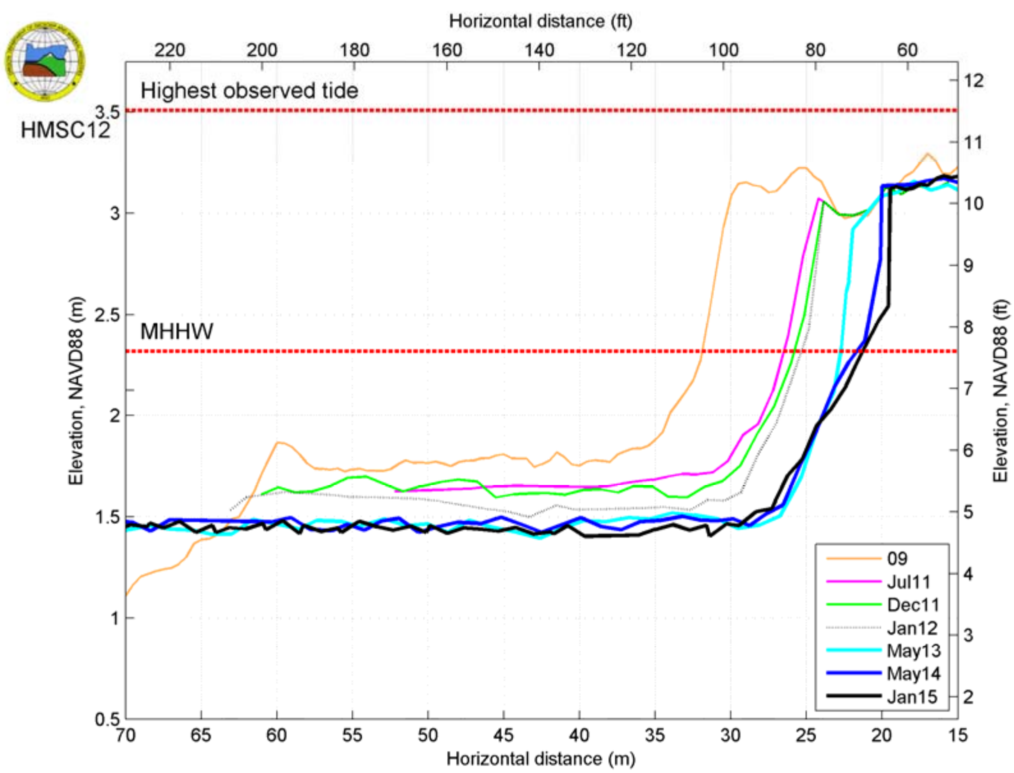

HMSC12
Horizontal distance (ft)
Highest observed tide
MHHW
Elevation, NAVD88 (m)
Elevation, NAVD88 (ft)
Horizontal distance (m)
09
Jul11
Dec11
Jan12
May13
May14
Jan15

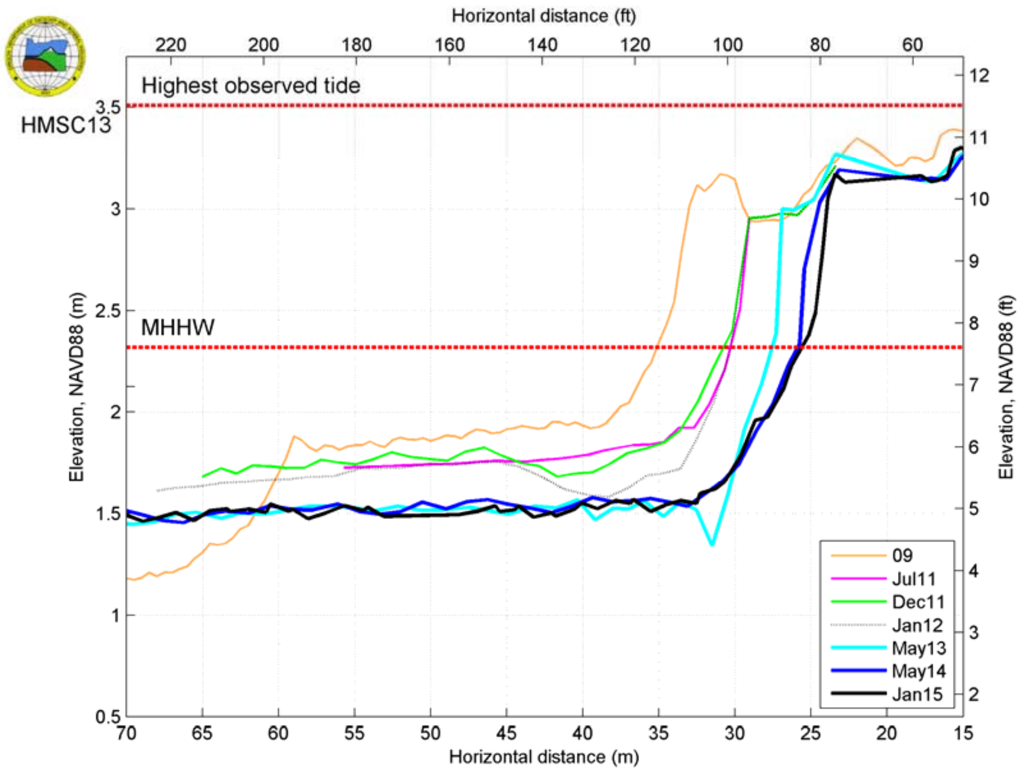
Horizontal distance (ft)
Highest observed tide
HMSC13
MHHW
Elevation, NAVD88 (m)
Elevation, NAVD88 (ft)
09
Jul11
Dec11
Jan12
May13
May14
Jan15
Horizontal distance (m)

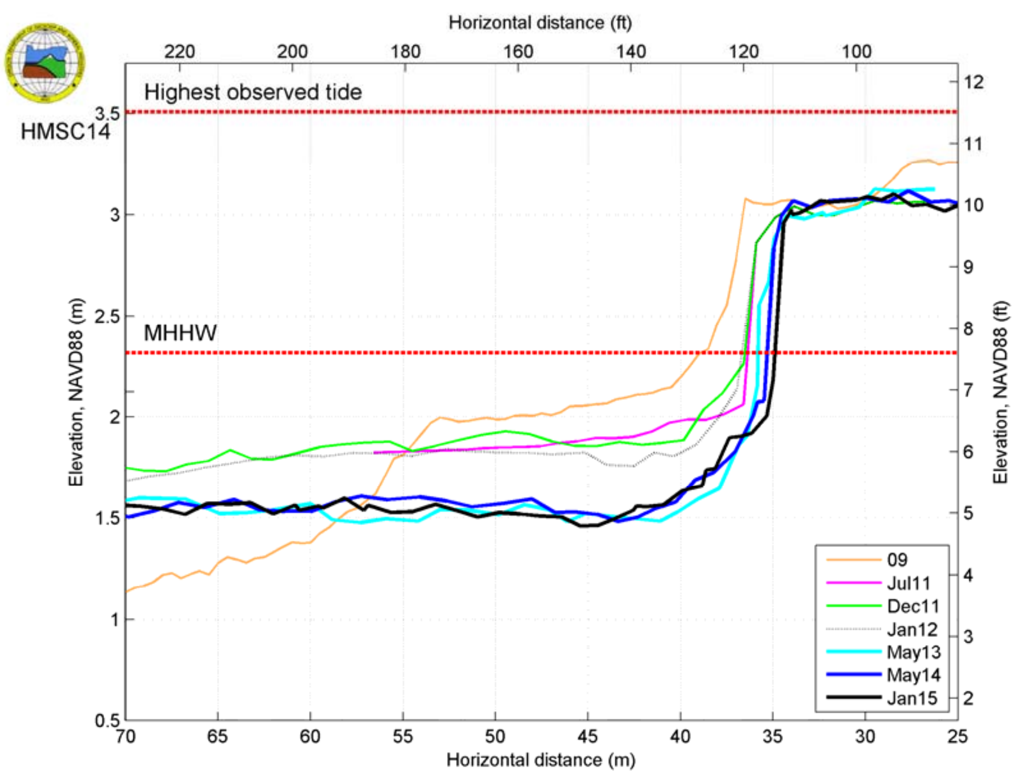
Horizontal distance (ft)
Highest observed tide
HMSC14
MHHW
Elevation, NAVD88 (m)
Elevation, NAVD88 (ft)
09
Jul11
Dec11
Jan12
May13
May14
Jan15
Horizontal distance (m)

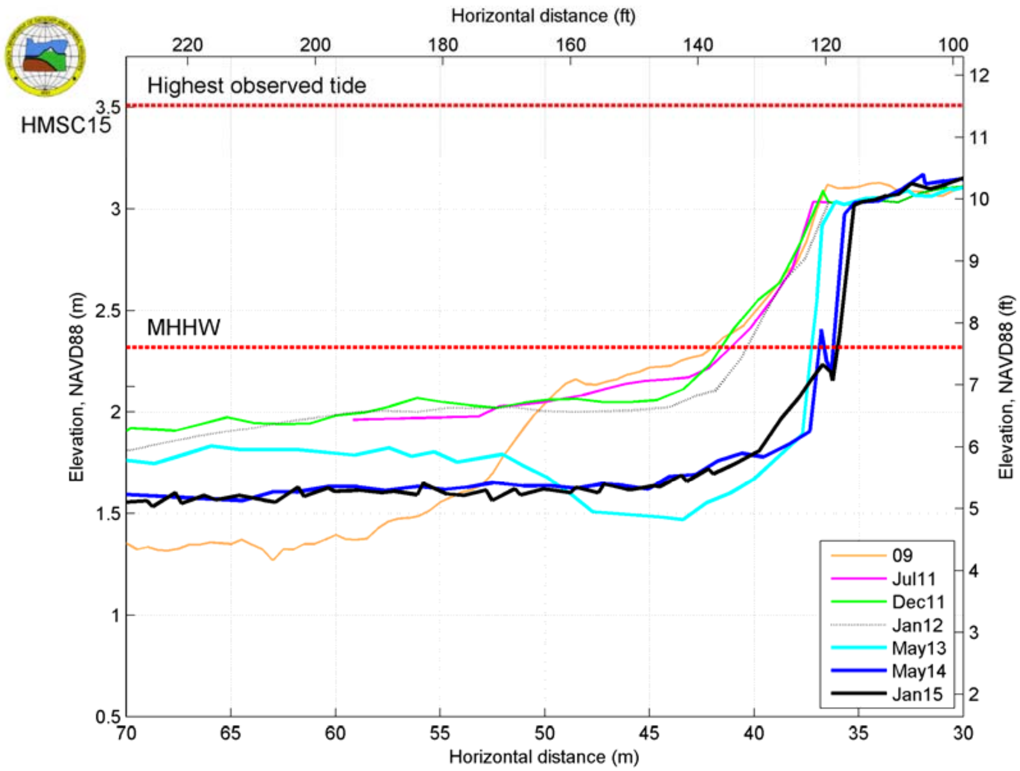
HMSC15
Horizontal distance (ft)
Highest observed tide
MHHW
Elevation, NAVD88 (m)
Elevation, NAVD88 (ft)
Horizontal distance (m)
09
Jul11
Dec11
Jan12
May13
May14
Jan15

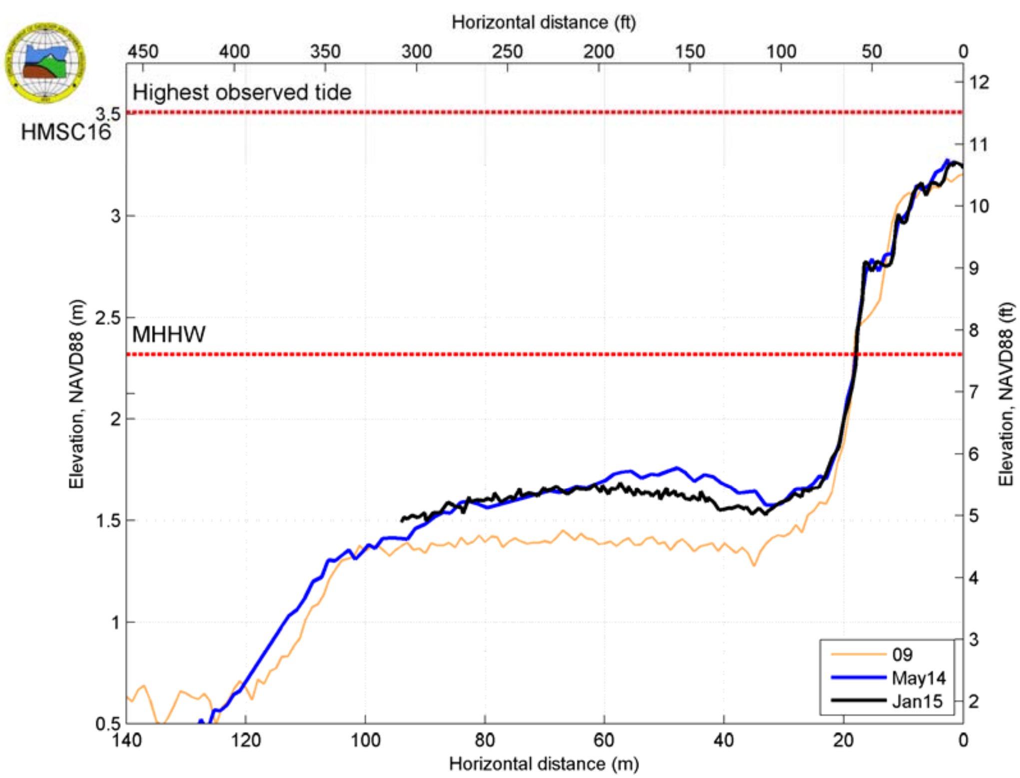
HMSC16
Horizontal distance (ft)
Highest observed tide
MHHW
Elevation, NAVD88 (m)
Elevation, NAVD88 (ft)
Horizontal distance (m)
09
May14
Jan15

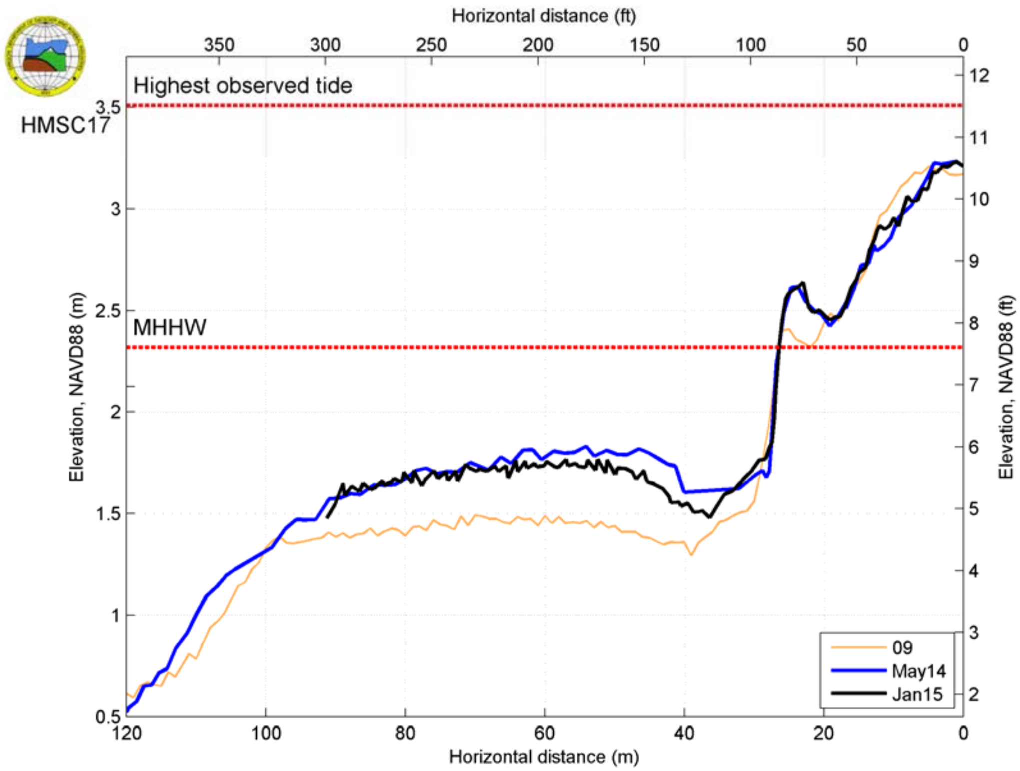
HMSC17
Horizontal distance (ft)
Highest observed tide
MHHW
Elevation, NAVD88 (m)
Elevation, NAVD88 (ft)
Horizontal distance (m)
09
May14
Jan15

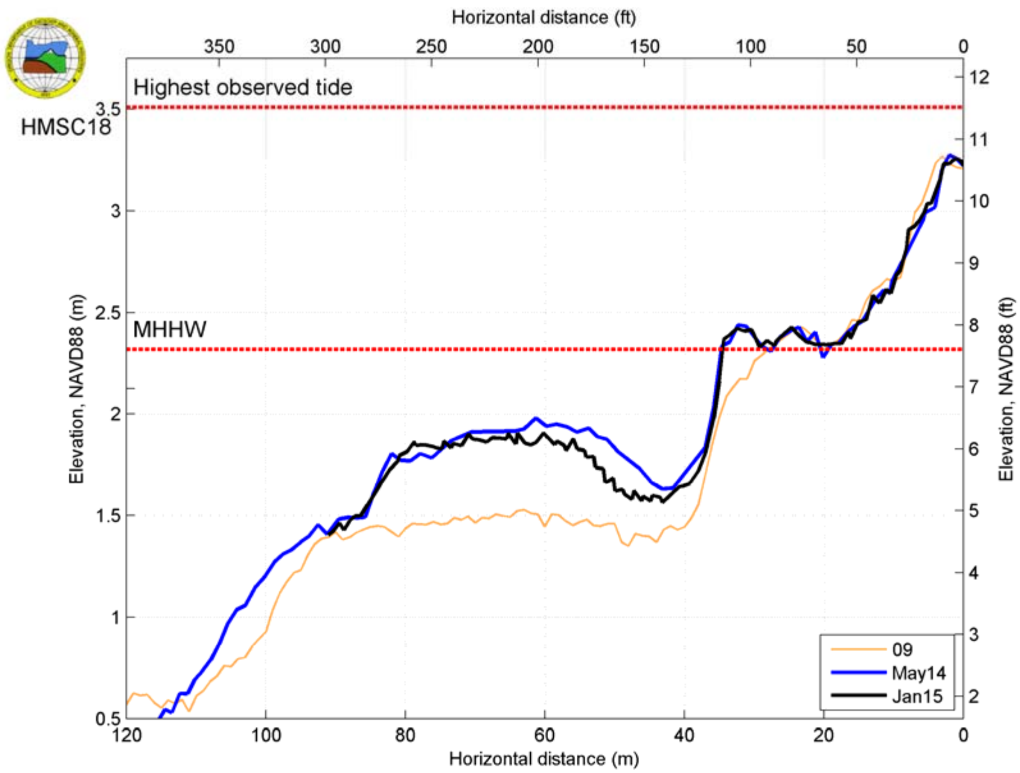
HMSC18
Horizontal distance (ft)
Highest observed tide
MHHW
Elevation, NAVD88 (m)
Elevation, NAVD88 (ft)
Horizontal distance (m)
09
May14
Jan15

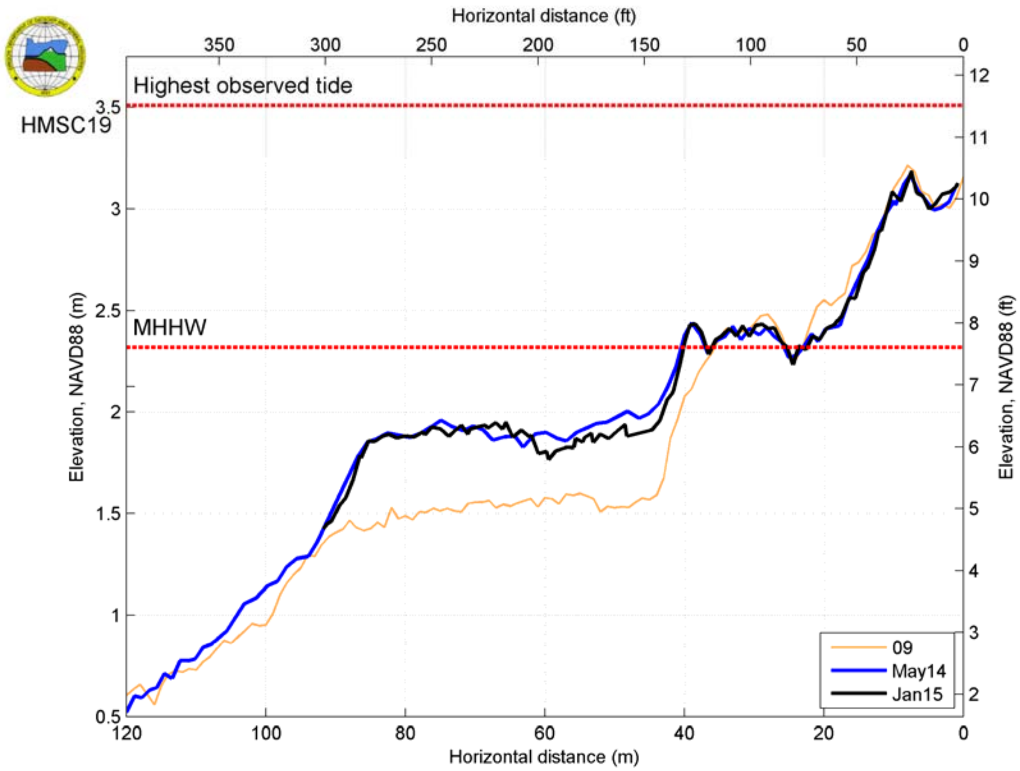
HMSC19
Horizontal distance (ft)
350
300
250
200
150
100
50
0
Highest observed tide
MHHW
Elevation, NAVD88 (m)
3.5
3
2.5
2
1.5
1
0.5
Elevation, NAVD88 (ft)
12
11
10
9
8
7
6
5
4
3
2
09
May14
Jan15
120
100
80
60
40
20
0
Horizontal distance (m)